A translation proofreader of archaeal origin imparts multialdehyde stress tolerance to land plants

Pradeep Kumar[1,2,3], Ankit Roy[1], Shivapura Jagadeesha Mukul[1,2,3], Avinash Kumar Singh[1], Dipesh Kumar Singh[1], Aswan Nalli[1], Pujaita Banerjee[1], Kandhalu Sagadevan Dinesh Babu[1], Bakthisaran Raman[1], Shobha P. Kruparani[1], Imran Siddiqi[1,2], Rajan Sankaranarayanan[1,2,3*]

[1]CSIR–Centre for Cellular and Molecular Biology, Uppal Road, Hyderabad 500007, India.
[2]Academy of Scientific and Innovative Research (AcSIR), CSIR–CCMB campus, Uppal Road, Hyderabad 500007, India

[3]Academy of Scientific and Innovative Research (AcSIR), Ghaziabad- 201002, India

***Corresponding author. Email: sankar@ccmb.res.in (RS)**

Abstract

Aldehydes, being an integral part of carbon metabolism, energy generation and signalling pathways, are ingrained in plant physiology. Land plants have developed intricate metabolic pathways which involve production of reactive aldehydes and its detoxification to survive harsh terrestrial environments. Here, we show that physiologically produced aldehydes i.e., formaldehyde and methylglyoxal in addition to acetaldehyde, generate adducts with aminoacyl-tRNAs, a substrate for protein synthesis. Plants are unique in possessing two distinct chiral proofreading systems, D-aminoacyl-tRNA deacylase1 (DTD1) and DTD2, of bacterial and archaeal origins, respectively. Extensive biochemical analysis revealed that only archaeal DTD2 can remove the stable D-aminoacyl adducts on tRNA thereby shielding archaea and plants from these system-generated aldehydes. Using Arabidopsis as a model system, we have shown that the loss of DTD2 gene renders plants susceptible to these toxic aldehydes as they generate stable alkyl modification on D-aminoacyl-tRNAs, which are recycled only by DTD2. Bioinformatic analysis identifies the expansion of aldehyde metabolising repertoire in land plant ancestors which strongly correlates with the recruitment of archaeal DTD2. Finally, we demonstrate that the overexpression of DTD2 offers better protection against aldehydes than in wild-type Arabidopsis highlighting its role as a multi-aldehyde detoxifier that can be explored as a transgenic crop development strategy.

Introduction

Reactive metabolites are an integral part of biological systems as they fuel a plethora of fundamental processes of life. Metabolically generated aldehydes are chemically diverse reactive metabolites such as formaldehyde (1-C), acetaldehyde (2-C) and methylglyoxal (MG; 3-C). Formaldehyde integrates various carbon metabolic pathways and is produced as a by-product of oxidative demethylation by various enzymes[1–6] whereas acetaldehyde is an intermediate of anaerobic fermentation[7]. Alternatively, MG is produced via the glycolysis pathway from dihydroxyacetone phosphate (DHAP) and glyceraldehyde-3-phosphate (G3P), oxidative deamination of glycine and threonine, fatty acid degradation and auto-oxidation of glucose inside the cell[8]. These aldehydes are involved in carbon metabolism[1–3,9,10], energy generation[7] and signalling[8,11], respectively, in all domains of life. In addition to the three aldehydes discussed above, plants also produce a wide range of other aldehydes under various biotic and abiotic stresses[8,12]. Despite their physiological importance, these aldehydes become genotoxic and cellular hazards at higher concentrations as they irreversibly modify the free amino group of various essential biological macromolecules like nucleic acids, proteins, lipids, and amino acids[13–17]. Increased levels of formaldehyde and MG leads to toxicity in various life forms like bacteria[18] and mammals[9,19,20]. However, archaea and plants possess these aldehydes in high amounts (>25-fold) (Figure: S1A), yet there is no evidence of toxicity[3,21–29]. This suggests that both archaea and plants have evolved specialised protective mechanisms against toxic aldehyde flux.

Using genetic screening Takashi *et al*. have identified a gene, called GEK1 at that time, essential for the protection of plants from ethanol and acetaldehyde[30,31]. Later, using biochemical and bioinformatic analysis, GEK1 was identified to be a homolog of archaeal D-aminoacyl-tRNA deacylase (DTD)[32]. DTDs are *trans* acting, chiral proofreading enzymes involved in translation quality control and remove D-amino acids mischarged onto tRNAs[33–37]. DTD function is conserved across all life forms where DTD1 is present in bacteria and eukaryotes, DTD2 in land plants and archaea[32,38] and DTD3 in cyanobacteria[39]. All DTDs are shown to be important in protecting organisms from D-amino acids[32,33,35,38,39]. In addition, DTD2 was also found to be involved in protecting plants against ethanol and acetaldehyde[30–32]. Recently, we identified the biochemical role of archaea-derived DTD2 gene in alleviating acetaldehyde stress in addition to resolving organellar incompatibility of bacteria derived DTD1 in land plants[40,41]. We have shown that acetaldehyde irreversibly modifies D-aminoacyl-tRNAs (D-aa-tRNA) and only DTD2 can recycle the modified D-aa-tRNAs thus replenishing

the free tRNA pool for further translation[40]. Like acetaldehyde, elevated aldehyde spectrum (Figure: S1A) in plants and archaea pose a threat to the translation machinery. The unique presence of DTD2 in organisms with elevated aldehyde spectrum (plants and archaea) and its indispensable role in acetaldehyde tolerance prompted us to investigate the role of archaeal DTD2 in safeguarding translation apparatus of plants from various physiologically abundant toxic aldehydes.

Here, our *in vivo* and biochemical results suggest that formaldehyde and MG lead to toxicity in DTD2 mutant plants through D-aa-tRNA modification. Remarkably, out of all the aldehyde-modified D-aa-tRNAs tested, only the physiologically abundant ones (i.e., D-aa-tRNAs modified by formaldehyde or methylglyoxal) were deacylated by both archaeal and plant DTD2s. Therefore, plants have recruited archaeal DTD2 as a potential detoxifier of all toxic aldehydes rather than only acetaldehyde as earlier envisaged. Furthermore, DTD2 overexpressing Arabidopsis transgenic plants demonstrate enhanced multi-aldehyde resistance that can be explored as a strategy for crop improvement.

Results

Aldehydes modify D-aa-tRNAs to disrupt protein synthesis

The presence of large amounts of chemically diverse aldehydes in plants and archaea (Figure: S1A) encouraged us to investigate their influence on aa-tRNAs, a key component of the translational machinery. We incubated aa-tRNAs with diverse aldehydes (from formaldehyde (1-C) to decanal (10-C) including MG (3-C)) and investigated adduct formation with thin-layer chromatography (TLC) and electrospray ionization mass spectrometry (ESI-MS). We observed that aldehydes modified aa-tRNAs irrespective of amino acid chirality (Figure: 1A-G; S1B). The mass change from formaldehyde, propionaldehyde, butyraldehyde and MG modification correspond to a methyl, propyl, butyl and acetonyl group, respectively (Figure: 1C-G). Tandem fragmentation (MS^2) of aldehyde-modified D-aa-tRNAs showed that all the aldehydes selectively modify only the amino group of amino acids in D-aa-tRNAs (Figure: S1C-G). Interestingly, upon a comparison of modification strength, the propensity of modification decreased with increase in the aldehyde chain length with no detectable modification on decanal treated aa-tRNAs (Figure: 1A, 1H). The chemical reactivity of aldehyde is dictated by its electrophilicity[42]. The electrophilicity of saturated aldehydes decreases with the increasing chain length of aldehyde[42,43], thereby reducing modification propensity. Exceptionally, the

modification propensity of MG is much higher than propionaldehyde (Figure: 1H) which is also a three carbon system (Figure: S1H) and it is likely due to the high electrophilicity of the carbonyl carbon[42]. Also, the aldehydes with higher propensity of modification are present in higher amounts in plants and archaea (Figure: S1A). Further, we investigated the effect of aldehyde modification on the stability of ester linkage of aa-tRNAs by treating them with alkaline conditions. Strikingly, even the smallest aldehyde modification stabilized the ester linkage by ~20-fold when compared with unmodified aa-tRNA (Figure: 1I-J).

Elongation factor thermo unstable (EF-Tu) is shown to protect L-aa-tRNAs from acetaldehyde modification[40]. EF-Tu based protection of L-aa-tRNAs can be extended to any aldehydes with similar or bigger size than acetaldehyde but not formaldehyde. We sought to investigate the elongation factor based protection against formaldehyde. To understand this, we have done a thorough sequence and structural analysis. We analysed the aa-tRNA bound elongation factor structure from bacteria (PDB ids: 1TTT) and found that the side chain of amino acid in the amino acid binding site of EF-Tu is projected outside (Figure: 2A; S2A). In addition, the amino group of amino acid is tightly selected by the main chain atoms of elongation factor thereby lacking a space for aldehydes to enter and then modify the L-aa-tRNAs and Gly-tRNAs (Figure: 2B; S2B). Modelling of D-amino acid (either D-phenylalanine or smallest chiral amino acid, D-alanine) in the same site shows serious clashes with main chain atoms of EF-Tu, indicating a D-chiral rejection during aa-tRNA binding by elongation factor (Figure: 2C-E). Next, we superimposed the tRNA bound mammalian (from *Oryctolagus cuniculus*) eEF-1A cryoEM structure (PDB id: 5LZS) with bacterial structure to understand the structural differences in terms of tRNA binding and found that elongation factor binds tRNA in a similar way (Figure: S2C-D). Modelling of D-alanine in the amino acid binding site of eEF-1A also shows serious clashes with main chain atoms, indicating a general theme of D-chiral rejection during aa-tRNA binding by elongation factor (Figure: 2F; S2E). Structure-based sequence alignment of elongation factor from bacteria, archaea and eukaryotes (both plants and mammals) shows a strict conservation of amino acid binding site (Figure: 2G). Minor differences near the amino acid side chain binding site (as indicated in Wolfson and Knight, FEBS Letters, 2005) might induce the amino acid specific binding differences, if any (Figure: S2F). However, those changes will have no influence when the D-chiral amino acid enters the pocket, as the whole side chain would clash with the active site. To confirm these structural and sequence analyses biochemically, bacterial EF-Tu (*Thermus thermophilus*) was used. EF-Tu was activated by exchanging the GDP with GTP. Activated EF-Tu protected L-aa-tRNAs

from RNase (Figure: S2G). Next, we generated the ternary complex of activated EF-Tu and aa-tRNAs and incubated with formaldehyde. Reaction mixture was quenched at multiple time points and modification was assessed using TLC. It has been seen that activated EF-Tu protected L-aa-tRNAs from smallest aldehyde suggesting that EF-Tu is a dedicated protector of L-aa-tRNAs from all the cellular metabolites (Figure: S2H). However, the lower affinity of D-aa-tRNAs with EF-Tu results in their modification under aldehyde flux. Accumulation of these stable aldehyde-modified D-aa-tRNAs will deplete the free tRNA pool for translation. Therefore, removal of aldehyde-modified D-aa-tRNAs is essential for cell survival.

DTD2 recycles aldehyde modified D-aa-tRNAs

Aldehyde-mediated modification on D-aa-tRNAs generated a variety of alkylated-D-aa-tRNA adducts (Figure: 1A; S1B). While we earlier showed the ability of DTD2 to remove acetaldehyde induced modification, we wanted to test whether it can remove diverse range of modifications ranging from smaller methyl to larger valeryl adducts to ensure uninterrupted protein synthesis in plants. To test this, we cloned and purified *Arabidopsis thaliana* (*At*) DTD2 and performed deacylation assays using different aldehyde-modified D-Tyr-(*At*)tRNA^{Tyr} as substrates. DTD2 cleaved majority of aldehyde modified D-aa-tRNAs at 50 pM to 500 nM range (Figure: 3A-D; S3A-B; S4A-F). Interestingly, DTD2's activity decreases with increase in aldehyde chain lengths (Figure: 3A-D; S3A-B; S4A-F). To establish DTD2's activity on various aldehyde modified D-aa-tRNAs as a universal phenomenon, we checked DTD2 activity from an archaeon [*Pyrococcus horikoshii* (*Pho*)]. DTD2 from archaea recycled short chain aldehyde-modified D-aa-tRNA adducts as expected (Figure: 3E-G) and, like DTD2 from plants, it did not act on aldehyde-modified D-aa-tRNAs longer than three carbons (Figure: 3H; S3C-D; S4G-L). Whereas the canonical chiral proofreader, DTD1, from plants was inactive on all aldehyde modified D-aa-tRNAs (Figure: 3I-L; S3E-F). Interestingly, DTD2 was inactive on butyraldehyde, and higher chain length aldehyde modified D-aa-tRNAs (Figure: 3D, 3H; S3A-D; S4D-F, S4J-L). This suggests that DTD2 exerts its protection till propionaldehyde with a significant preference for methylglyoxal and formaldehyde modified D-aa-tRNAs. It is worth noting that the physiological levels of higher chain length aldehydes are comparatively much lesser in plants and archaea (Figure: S1A), indicating the coevolution of DTD2 activity with the presence of toxic aldehydes. Even though both MG and propionaldehyde generate a 3-carbon chain modification, DTD2 showed ~100-fold higher activity on MG-modified D-aa-tRNAs (Figure: 3B-C, 3F-G, 3M). It is interesting to note that peptidyl-tRNA hydrolase (PTH),

which recycles on N-acetyl/peptidyl-L-aa-tRNAs and has a similar fold to DTD2, was inactive on formaldehyde and MG-modified L- and D-aa-tRNAs (Figure: 3M; S4M-Q). Overall, our biochemical assays with multiple *trans* acting proofreaders (DTD1 and DTD2) and peptidyl-tRNA recycling enzymes (both bacterial and archaeal PTH) suggests that DTD2 is the only aldehyde detoxifier recycling the tRNA pool in both plants and archaea.

Absence of DTD2 renders plants susceptible to physiologically abundant toxic aldehydes

Biochemical assays suggest that DTD2 may exert its protection for both formaldehyde and MG in addition to acetaldehyde. To test this *in vivo*, we utilised an *A. thaliana* T-DNA insertion line (SAIL_288_B09) having T-DNA in the first exon of DTD2 gene (Figure: 4A). We generated a homozygous line (Figure: 4A) and checked them for ethanol sensitivity as ethanol metabolism produces acetaldehyde. Similar to earlier results[30–32], dtd2-/- (*dtd2* hereafter) plants were susceptible to ethanol (Figure: S5A) confirming the non-functionality of *DTD2* gene in *dtd2* plants. We then subjected them to various concentrations of formaldehyde and MG generally used for plant toxicity assays[44–46]. These *dtd2* plants were found to be sensitive to both formaldehyde and MG (Figure: 4B-G). This sensitivity was alleviated by complementing *dtd2* mutant line with genomic copy of wild type DTD2 (Figure: 4A-G), indicating that DTD2-mediated detoxification plays an important role in plant aldehyde stress. To further confirm the significance of DTD2 in plant growth and development, we performed seed germination assays in *dtd2* plants by evaluating the emergence of radicle on 3rd day post seed plating. As expected, *dtd2* plants show a significant reduction (~40%) in germination (Figure: 4H-I) and this effect was reversed in the DTD2 rescue line (Figure: 4H-I). Interestingly, these toxic effects (on both growth and germination) of formaldehyde and MG were enhanced upon D-amino acid supplementation (Figure: S5B). These observations suggest that DTD2's chiral proofreading activity is associated with aldehyde stress removal activity as well. Moreover, to rule out the plausible role of any interacting partner or any other indirect role of DTD2, we generated a catalytic mutant transgenic line containing a genomic copy of *At*DTD2 having H150A mutation[38] (Figure: S5C-F). The catalytic mutant line showed a similar phenotype as *dtd2* plants under aldehyde stress (Figure: 4A-I), confirming the role of DTD2's biochemical activity in relieving general aldehyde toxicity in plants. We tried to characterise the aldehyde modified D-aminoacyl adducts on tRNAs with *dtd2* mutant plants extensively through Northern blotting as well as mass spectrometry. However, due to the lack of information about the tissue getting affected (root, shoot etc.), identity of aa-tRNA as well as location of aa-tRNA

(cytosol or organellar), we are so far unsuccessful in identifying them from plants. However, we have used a bacterial surrogate system, *E. coli*, as used earlier[40] to show the accumulation of D-aa-tRNA adducts in the absence of DTD protein. We could identify the accumulation of both formaldehyde and MG modified D-aa-tRNA adducts via mass spectrometry (Figure: S6A-H). Overall, our results show that DTD2-mediated detoxification protects plants from physiologically abundant toxic aldehydes.

Overexpression of DTD2 provides enhanced multi-aldehyde stress-tolerance to plants

Plants being sessile are constantly subjected to multiple environmental stresses that reduce agriculture yield and constitute a serious danger to global food security[47]. Pyruvate decarboxylase (PDC) transgenics are used to increase flood tolerance in plants but it produces ~35-fold higher acetaldehyde than wild-type plants[48]. Transgenics overexpressing enzymes known for aldehyde detoxification like alcohol dehydrogenase (ADH), aldehyde dehydrogenase (ALDH), aldehyde oxidase (AOX) and glyoxalase are shown to be multi-stress tolerant[49–52]. The sensitivity of *dtd2* plants under physiological aldehydes and biochemical activity of DTD2 prompted us to check if overexpression of DTD2 can provide multi-aldehyde tolerance. We generated a DTD2 overexpression line with DTD2 cDNA cloned under a strong CaMV 35S promoter[53]. We subjected the overexpression line, along with the wild type, to various aldehydes with or without D-amino acids. Strikingly, we found that the DTD2 overexpression line was more tolerant to both the aldehydes (formaldehyde and MG) when compared with wild type (Figure: 5A-C; S7A-C). DTD2 overexpression resulted in >50% increased seedling growth when compared with that of wild type (Figure: 6A; S7D). The growth difference was more pronounced when D-amino acids were supplemented with varying concentrations of aldehydes (Figure: 5A; S7D). Interestingly, DTD2 overexpression plants showed extensive root growth under the influence of both formaldehyde and MG (Figure: S7A-C). Plants produce these aldehydes in huge amounts under various stress conditions[12,26] and plant tolerance to various abiotic stresses is strongly influenced by root growth[54]. The enhanced root growth by DTD2 overexpression under aldehyde stress imply that DTD2 overexpression offers a viable method to generate multi-stress-resistant crop varieties.

DTD2 appearance corroborates with the aldehyde burst in land plant ancestors

After establishing the role of DTD2 as a general aldehyde detoxification system in the model land plant system, we wondered if the multi aldehyde detoxification potential of DTD2 was

present in land plant ancestors as well. Therefore, we checked the biochemical activity of DTD2 from a charophyte algae, *Klebsormedium nitens* (*Kn*), and found that it also recycled aldehyde-modified D-aa-tRNAs adducts like other plant and archaeal DTD2s (Figure: 6A-C; S8A-C). This suggests that the multi-aldehyde problem in plants has its roots in their distant ancestors, charophytes. Next, we analysed the presence of other aldehyde metabolizing enzymes across plants. Multiple bioinformatic analyses have shown that land plants encode greater number of ALDH genes compared to green algae[55,56] and glyoxalase family (GlyI, GlyII and GlyIII), known to clear MG, has expanded exclusively in streptophytic plants[57,58]. We identified that land plants also encode greater number of AOX genes in addition to ALDH genes compared to green algae (Figure: S8D). We delved deeper into plant metabolism with an emphasis on formaldehyde and MG. A search for the formaldehyde (C00067) and MG (C00546) in KEGG database[59] have shown that formaldehyde is involved in 5 pathways, 60 enzymes, and 94 KEGG reactions, while MG in 6 pathways, 16 enzymes and 16 KEGG reactions. We did a thorough bioinformatic search for the presence of around 31 and 9 enzymes related to formaldehyde and MG, respectively, in KEGG database (Table: S2). Strikingly, we found that plants encode majority of the genes related for formaldehyde and MG and they are conserved throughout land plants (Figure: 6D; S8E-G) (Table: S2). Plants produce significant amounts of formaldehyde while reshuffling pectin in their cell wall during cell division, development and tissue damage[60,61]. Plants contain ~33% pectin in their cell walls that provides strength and flexibility[62]. When checked for the presence of genes responsible for the pectin biosynthesis and degradation, we identified that it is a land plant specific adaptation that originated in early diverging streptophytic algae (Figure: S8F) (Table: S2). Overall, our bioinformatic analysis in addition to earlier studies have identified an expansion of aldehyde metabolising repertoire in land plants and their ancestors indicating the sudden aldehyde burst accompanying terrestrialization which strongly correlates with the recruitment of DTD2 (Figure: 6E; 7).

Discussion

Plants produce more than two-hundred thousand metabolites for crosstalk with other organisms[63]. The burgeoning information on increased utilization of aldehydes for signalling, defence and altering the ecological interactions with other organisms suggests their physiological importance in plant life[26]. However, aldehydes are strong electrophiles that undergo addition reactions with amines and thiol groups to form toxic adducts with

biomolecules. Excessive aldehyde accumulation irreversibly modifies nucleic acids and proteins resulting in cell death[17,19]. In this work, we have shown that multiple aldehydes can cause toxicity in *dtd2* plants. Therefore, plants have recruited DTD2 as a detoxifier of aldehyde-induced toxicities in the context of protein biosynthesis. Through this work, we find a correlation between physiological abundance of various aldehydes, their modification propensity and DTD2's aldehyde protection range. Aldehydes with higher reactivity (formaldehyde, acetaldehyde and MG) are present in higher amounts in plants and archaea and DTD2 provides modified-D-aa-tRNA deacylase activity against these aldehydes. DTD2's biochemical activity decreases with increase in the aldehyde chain length. Intriguingly, despite MG and propionaldehyde generating a 3-carbon long modification, DTD2 is ~100-fold more active on MG-modified D-aa-tRNAs. The absence of carbonyl carbon in the propionaldehyde-modified substrate and DTD2's preferential activity on the bulkier MG modified substrate points to a clear evolutionary selection pressure for the abundant and physiologically relevant aldehyde. In total contrast to DTD2, all PTH substrates contain carbonyl carbon at the alpha position after the amino group of amino acid in L-aa-tRNA[64]. The inactivity of PTH on MG modified L- and D-aa-tRNAs suggests its specificity for carbonyl carbon at alpha position (Figure: S4Q). Therefore, elucidating the structural basis for both enantioselection and modification specificity of DTD2 and PTH will throw light on these key mechanisms during translation quality control.

The sensitivity of *dtd2* plants to aldehydes of higher prevalence and hyper-propensity for modification indicates the physiological coevolution of aldehyde phytochemistry and recruitment of DTD2 in land plants. Despite the toxic effects of reactive aldehydes, plants are being used as air purifiers as they act as aldehyde scavengers from the environment[65–68]. Moreover, plants have higher removal rates for formaldehyde and acetaldehyde as compared to other higher chain length aldehydes from the environment[68]. These aldehydes are produced under various biotic and abiotic stresses in plants and overexpression of enzymes (PDC, ADH, ALDH and glyoxalase) involved in aldehyde detoxification are shown to provide multi-stress tolerance[49,69–71]. In similar lines, here, we have also explored the possibility of DTD2 overexpression in multi-aldehyde stress tolerance. Our *in vivo* results strongly suggests that DTD2 provides multi-aldehyde stress tolerance in the context of detoxifying adducts formed on aa-tRNA. This facilitates the release of free tRNA pool thus relieving translation arrest. DTD2 overexpression plants showed extensive root growth as compared to wildtype plants.

Plant root growth is an indicator of multi-stress tolerance[54]. Therefore, our DTD2 overexpression approach could be explored further in crop improvement strategies.

The role of reactive aldehydes like formaldehyde in the origin of life is inevitable[72]. The presence of reactive aldehydes[73,74] and D-amino acids[75,76] for such a long time suggests an ancient origin of DTD2 activity in last archaeal common ancestor. As archaea thrivess in extreme conditions, they secrete enormous amount of formaldehyde into the environment as they grow[77]. We have shown that DTD2 from archaea can efficiently recycle physiologically abundant toxic aldehyde-modified D-aa-tRNAs like plant DTD2s. The adduct removal activity was utilised by the archaeal domain as they produce more aldehydes and thrive in harsh environments[78–80] and it was later acquired by plants. Bog ecosystems, earlier proposed site for DTD2 gene transfer[40], are highly anaerobic, rich in D-amino acids and ammonia[81–83], which lead to enhanced production of aldehydes (acetaldehyde[7] and MG[84]) in their inhabitants. Our bioinformatic analysis in addition to earlier studies[55–58] have identified an expansion of aldehyde metabolising repertoire exclusively in land plants and their ancestors indicating a sudden aldehyde burst associated with terrestrialization. Thus, recruitment of archaeal DTD2 by a land plant ancestor must have aided in the terrestrialization of early land plants. Considering the fact that there are no common incidences of archaeal gene transfer to eukaryotes, it is unclear whether the DTD2 gene was transferred directly to land plant ancestor from archaea or perhaps was mediated by an unidentified intermediate bacterium warrants further investigation. Overall, the study has established the role of archaeal origin DTD2 in land plants by mitigating the toxicity induced by aldehydes during protein biosynthesis.

Materials and methods

Plant material and growth conditions

Arabidopsis seeds of Columbia background were procured from the Arabidopsis Biological Resource Center (Col-0: CS28166; *dtd2*: SAIL_588_B09 [CS825029]). Plants were cultivated in a growth room at 22°C with 16 h of light. Seeds were germinated on 1× Murashige–Skoog (MS) medium plates containing 4.4 g/L MS salts, 20 g/L sucrose, and 8 g/L tissue culture agar with pH 5.75 adjusted with KOH at 22°C in a lighted incubator. Table S1 contains the primers used to genotype the plants via polymerase chain reaction (PCR).

Construction of DTD2 rescue and DTD2 overexpression line

The coding sequence for Arabidopsis DTD2 (At2g03800) was PCR amplified and inserted into pENTR/D-TOPO for the overexpression line and genomic sequence for DTD2 (At2g03800) along with its promoter (~2.4 kb upstream region of DTD2 gene) was PCR amplified and inserted into pENTR/D-TOPO for the rescue line (primer sequences available in Table S1). Site-directed mutagenesis approach was used to create H150A (catalytic mutant) in plasmid used for rescue line. LR Clonase II (Thermo Fisher Scientific) was used to recombine entry plasmids into a) pH7FWG2 to create the p35S::DTD2 line and b) pZP222 to create rescue and catalytic mutant line. *Agrobacterium tumefaciens* Agl1 was transformed with the above destination plasmids. The floral dip technique was then used to transform Arabidopsis plants with a Columbia background[85]. The transgenic plants for overexpression were selected with 50 µg/ml hygromycin and 1 µg/ml Basta (Glufosinate ammonium) and rescue plant lines with 120 µg/ml gentamycin and 1 µg/ml Basta (Glufosinate ammonium) supplemented with MS media.

Aldehyde sensitivity assays and seedling size quantification

For aldehyde sensitivity assays, seeds were initially sterilised with sterilisation solution and plated on 1× Murashige–Skoog (MS) medium agar plates containing varying concentrations of aldehydes with or without D-Tyrosine. Seeds were grown in a growth room at 22°C with 16 h of light. Plates were regularly observed and germination percentage was calculated based on the emergence of radicle on 3rd day post seed plating. Phenotypes were documented 2 weeks post germination and seedling size (n=4-15) was quantified. For seedling size quantification imaging was done using Axiozoom stereo microscope with ZEN 3.2 (blue edition) software and processed as necessary.

Total RNA extraction and reverse transcriptase-quantitative polymerase chain reaction

For the reverse transcriptase-quantitative polymerase chain reaction (RT-qPCR) experiment, seeds were germinated and grown for 14 days on MS plate and 200 mg of seedings were flash-frozen in liquid nitrogen. The RNeasy Plant Minikit (QIAGEN) was used to extract total RNA according to the manufacturer's instructions. 4 μg of total RNA was used for cDNA synthesis with PrimeScript 1st strand cDNA Synthesis Kit (Takara), according to the manufacturer's instructions. The resultant cDNA was diluted and used as a template for the RT-PCR reactions for DTD2 rescue and catalytic mutant lines with EF-Tu (At1g07920) as the internal control. While qPCR was done to quantify the level of DTD2 overexpression for DTD2 overexpression line with appropriate primers (Table S1) and Power SYBR™ Green PCR Master Mix (ThermoFisher). Reactions were carried out in a Bio-Rad CFX384 thermocycler, with three technical replicates per reaction. The $2^{-\Delta Cq}$ method was used for relative mRNA levels calculation with actin (At2g37620) as the internal control. Prism 8 was used for graph generation and statistical analysis.

Cloning, expression, and purification

DTD1 and DTD2 genes from *Arabidopsis thaliana* (*At*) were PCR–amplified from cDNA, and DTD2 gene from *Klebsormedium nitens* (*Kn*) was custom synthesised, while DTD2 gene from *Pyrococcus horikoshii* (*Pho*), and tyrosyl-tRNA synthetase (TyrRS) of *Thermus thermophilus* (*Tth*) were PCR-amplified using their genomic DNA with primers listed in table S1. All the above mentioned genes were then cloned into the pET28b vector via restriction-free cloning[86]. *E. coli* BL21(DE3) was used to overexpress all the above cloned genes except *Ec*PheRS where *E. coli* M15 was used. As Plant DTD2s, TyrRS, and PheRS contained 6X His-tag, they were purified via Ni-NTA affinity chromatography, followed by size exclusion chromatography using a Superdex 75 column (GE Healthcare Life Sciences, USA). Cation exchange chromatography (CEC) was used to purify *Pho* DTD2 no-tag protein followed by SEC. Purification method and buffers for all the purifications were used as described earlier[87]**.** All the purified proteins were stored in buffer containing 100 mM Tris (pH 8.0), 200 mM NaCl, 5 mM 2-mercaptoethanol (β-ME), and 50% Glycerol for further use.

Generation of α-^{32}P-labeled aa-tRNAs

We have used *A. thaliana* (*At*) $tRNA^{Phe}$, *A. thaliana* (*At*) $tRNA^{Tyr}$, and *E. coli* (*Ec*) $tRNA^{Ala}$ in this study. All the tRNAs were *in vitro* transcribed (IVT) using the MEGAshortscript T7 Transcription Kit (Thermo Fisher Scientific, USA). tRNAs were then radio labelled with [α-^{32}P] ATP (BRIT-Jonaki, India) at 3'-end using *E. coli* CCA-adding enzyme[88]. Aminoacylation

of $tRNA^{Phe}$, $tRNA^{Tyr}$, and $tRNA^{Ala}$ with phenylalanine, tyrosine, and alanine respectively, were carried out as mentioned earlier[87,89]. Thin-layer chromatography was used to quantify the aminoacylation as explained[40].

Generation of adducts on aa-tRNAs for probing relative modification propensity of aldehyde with aa-tRNA and substrate generation for biochemical activity

A single-step method was used for probing relative modification propensity of the aldehyde with aa-tRNA where 0.2 µM of Ala-$tRNA^{Ala}$ was incubated with different concentrations of aldehydes (2 mM, and 10 mM) along with 20 mM $NaCNBH_3$ (in 100 mM Potassium acetate (pH 5.4)) as a reducing agent at 37°C for 30 minutes**.** The reaction mixture was digested with S**1** nuclease and analysed on thin layer chromatography (TLC). Except for decanal, all the aldehydes modified Ala-$tRNA^{Ala}$. The method for processing and quantification of modification on aa-tRNA utilised is discussed earlier[40]. However, a two-step method was used for generating substrates for biochemical assays as discussed earlier[40]. It was used to generate maximum homogenous modification on the aa-tRNAs for deacylation assays. Briefly, 2 µM aa-tRNAs were incubated with 20 mM of formaldehyde, and methylglyoxal or 1M of propionaldehyde, butyraldehyde, valeraldehyde, and isolvaleraldehyde at 37°C for 30 minutes. Samples were dried to evaporate excess aldehydes using Eppendorf 5305 Vacufuge plus Concentrator. The dried mixture was then reduced with 20 mM $NaCNBH_3$ at 37°C for 30 minutes. All reactions were ethanol-precipitated at -30°C overnight or -80°C for 2 Hrs. Ethanol precipitated pellets were resuspended in 5 mM sodium acetate (pH 5.4) and used for biochemical assays.

Deacylation assays

For biochemical activity assays, various enzymes like DTD1s, DTD2s and PTHs were incubated with different aldehyde modified and unmodified α-^{32}P-labelled D-Tyr-$tRNA^{Tyr}$ substrates (0.2 µM) in deacylation buffer (20 mM Tris pH 7.2, 5 mM $MgCl_2$, 5 mM DTT, and 0.2 mg/ml bovine serum albumin) at 37°C. An aliquot of 1 µl of the reaction mixture was withdrawn at various time points and digested with S1 nuclease prior to their quantification by TLC. The quantity of aldehyde modified Tyr-AMP at t=0 min was considered as 100% and the the amount of modified Tyr-AMP at each time point normalised with respect to t=0 min was plotted. All biochemical experiments were repeated at least 3 times. The mean values of three independent observations were used to plot the graphs with each error bar representing the standard deviation from the mean value.

Alkali treatment

Both aldehyde modified and unmodified D-aa-tRNAs were digested with S1 nuclease before subjecting to alkali treatment (For formaldehyde: 100 nM S1-digested sample with 100 mM Tris pH 9.0; For methylglyoxal: 100 nM S1-digested sample with 200 mM Tris pH 9.0) at 37°C. Alkali-treated samples withdrawn at different time points were directly analysed with TLC. GraphPad Prism software was used to calculate the half-life by fitting the data points onto the curve based on the first-order exponential decay equation $[S_t] = [S_0]e^{-kt}$, where the substrate concentration at time t is denoted as $[S_t]$, $[S_0]$ is the concentration of the substrate at time 0, and k is the first-order decay constant.

Mass spectrometry (MS)

To identify the modification by various aldehydes on D-aa-tRNAs, modified and unmodified D-Phe-tRNA^{Phe} were digested with aqueous ammonia (25% of v/v NH_4OH) at 70°C for 18 hours[40]. Hydrolysed samples were dried using Eppendorf 5305 Vacufuge plus Concentrator. Dried samples were resuspended in 10% methanol and 1% acetic acid in water and analysed via ESI-based mass spectrometry using a Q-Exactive mass spectrometer (Thermo Scientific) by infusing through heated electrospray ionization (HESI) source operating at a positive voltage of 3.5 kV. Targeted selected ion monitoring (t-SIM) was used to acquire the mass spectra (at a resolving power of 70000@200m/z) with an isolation window of 2 m/z i.e., theoretical m/z and MH+ ion species. The high energy collision-induced (HCD) MS-MS spectra with a normalized collision energy of 25 of the selected precursor ion species specified in the inclusion list (having the observed m/z value from the earlier t-SIM analysis) were acquired using the method of t-SIM-ddMS2 (at an isolation window of 1 m/z at a ddMS2 resolving power of 35000@200m/z).

Characterisation of D-aa-tRNA adducts from *E. coli*

To identify the accumulation of D-aa-tRNA adducts, overnight grown primary culture of DTD1 knockout *E. coli* was used to inoculate 1% secondary culture in minimal media with or without 2.5 mM D-tyrosine. Secondary culture grown to OD_{650} (optical density at 650 nm) 0.8 was subjected to respective aldehyde treatment (0.01% final concentration) with 0.5 mM $NaCNBH_3$ at 37°C for 30 minutes. Cultures were pelleted and total RNA was isolated through acidic phenol chloroform method. Total RNA was digested with 3 volumes of aqueous ammonia (25% of v/v NH_4OH) at 70°C for 18 hours[40]. Hydrolysed samples were dried using Eppendorf 5305 Vacufuge plus Concentrator. Dried samples were resuspended in 10% methanol and 1%

acetic acid in water and analysed via ESI-based mass spectrometry using a Q-Exactive mass spectrometer (Thermo Scientific) as mentioned above.

Bioinformatic analysis

Protein sequences for various enzymes involved in formaldehyde and MG metabolism were searched in KEGG GENOME database (http://www.genome.jp/kegg/genome.html) (RRID: SCR_012773) through KEGG blast search and all blast hits were mapped on KEGG organisms to identify their taxonomic distribution. KEGG database lacks genome information for charophyte algae so the presence of desired enzymes in charophyte was identified by blast search in NCBI (https://www.ncbi.nlm.nih.gov/) (RRID: SCR_006472). Protein sequences for elongation factor (both EF-Tu and eEF-1a) for the representative organisms were downloaded from NCBI through BLAST-based search. The structure-based multiple sequence alignment of elongation factor was prepared using the T-coffee (http://tcoffee.crg.cat/) (RRID: SCR 011818) server, and the sequence alignment figure was generated using ESPript 3.0 (http://espript.ibcp.fr/ESPript/cgi-bin/ESPript.cgi).

Structure models for elongation factor complexed with aa-tRNA were downloaded from RCSB-PDB (https://www.rcsb.org/) and analysed with The PyMOL Molecular Graphics System, Version 2.0 Schrödinger, LLC. 'ProteinInteractionViewer' plugin for Pymol was used with default parameters to identify and represent the molecular clashes in elongation factor structures with L-Phenylalanine and modelled D-Phenylalanine, L- and D-alanine in the amino acid binding site of elongation factor. Figures were prepared with The PyMOL Molecular Graphics System, Version 2.0 Schrödinger, LLC.

Quantification and statistical analysis

Quantification approaches and statistical analyses of the deacylation assays can be found in the relevant sections of the Methods section.

Author Contributions:

Conceptualization: P.K., R.S.

Methodology: P.K., A.R., D.K.S., S.P.K., R.S.

Investigation: P.K., A.R., S.J.M., A.K.S., A.N., P.B., K.S.D.B., B.R.

Visualization: P.K., A.R., S.J.M.

Supervision: R.S., I.S.

Writing—original draft: P.K., R.S.

Writing—review & editing: P.K., R.S., S.J.M., A.R., S.P.K., I.S., D.K.S., P.B., K.S.D.B., A.N., A.K.S., B.R.

Acknowledgments

The authors acknowledge Dr. Mukesh Lodha, CSIR-CCMB for fruitful discussions and Gokulan C G, CSIR-CCMB for qRT-PCR related help. PK and SJM thank CSIR, India for research fellowship. RS acknowledges healthcare theme project (MLP-0162, MLP-0138), CSIR, India, J.C. Bose Fellowship of SERB, India, and Centre of Excellence Project (GAP-0473) of Department of Biotechnology, India.

Competing interests

Authors declare no competing interests.

Reference

1. Jardine, K. J. *et al.* Integration of C_1 and C_2 Metabolism in Trees. *Int. J. Mol. Sci.* **18**, 2045 (2017).

2. Song, Z.-B. *et al.* C1 metabolism and the Calvin cycle function simultaneously and independently during HCHO metabolism and detoxification in Arabidopsis thaliana treated with HCHO solutions. *Plant. Cell Environ.* **36**, 1490–1506 (2013).

3. Trézl, L., Hullán, L., Szarvas, T., Csiba, A. & Szende, B. Determination of Endogenous Formaldehyde in Plants (Fruits) Bound to L-Arginine and its Relation to the Folate Cycle, Photosynthesis and Apoptosis. *Acta Biol. Hung.* **49**, 253–263 (1998).

4. Loenarz, C. & Schofield, C. J. Expanding chemical biology of 2-oxoglutarate oxygenases. *Nat. Chem. Biol.* **4**, 152–156 (2008).

5. Shi, Y. *et al.* Histone demethylation mediated by the nuclear amine oxidase homolog LSD1. *Cell* **119**, 941–953 (2004).

6. Walport, L. J., Hopkinson, R. J. & Schofield, C. J. Mechanisms of human histone and nucleic acid demethylases. *Curr. Opin. Chem. Biol.* **16**, 525–534 (2012).

7. Tadege, M. & Kuhlemeier, C. Aerobic fermentation during tobacco pollen development. *Plant Mol. Biol.* **35**, 343–354 (1997).

8. Mostofa, M. G. *et al.* Methylglyoxal - a signaling molecule in plant abiotic stress responses. *Free Radic. Biol. Med.* **122**, 96–109 (2018).

9. Burgos-Barragan, G. *et al.* Mammals divert endogenous genotoxic formaldehyde into one-carbon metabolism. *Nature* **548**, 549–554 (2017).

10. Hill, P. W. *et al.* Acquisition and assimilation of nitrogen as peptide-bound and D-enantiomers of amino acids by wheat. *PLoS One* **6**, e19220 (2011).

11. Kosmachevskaya, O. V., Shumaev, K. B. & Topunov, A. F. Signal and regulatory

effects of methylglyoxal in eukaryotic cells. *Appl. Biochem. Microbiol.* **53**, 273–289 (2017).

12. Jardine, K. *et al.* Carbon isotope analysis of acetaldehyde emitted from leaves following mechanical stress and anoxia. *Plant Biol.* **11**, 591–597 (2009).

13. Seitz, H. K. & Stickel, F. Molecular mechanisms of alcohol-mediated carcinogenesis. *Nat. Rev. Cancer* **7**, 599–612 (2007).

14. Fang, J. L. & Vaca, C. E. Detection of DNA adducts of acetaldehyde in peripheral white blood cells of alcohol abusers. *Carcinogenesis* **18**, 627–632 (1997).

15. Matsuda, T. *et al.* Effective utilization of N2-Ethyl-2′-deoxyguanosine triphosphate during DNA synthesis catalyzed by mammalian replicative DNA polymerases. *Biochemistry* **38**, 929–935 (1999).

16. Fang, J. L. & Vaca, C. E. Development of a 32P-postlabelling method for the analysis of adducts arising through the reaction of acetaldehyde with 2’-deoxyguanosine-3’-monophosphate and DNA. *Carcinogenesis* **16**, 2177–2185 (1995).

17. Carlsson, H., Stedingk, H. von, Nilsson, U. & Törnqvist, M. LC–MS/MS Screening Strategy for Unknown Adducts to N-Terminal Valine in Hemoglobin Applied to Smokers and Nonsmokers. *Chem. Res. Toxicol.* **27**, 2062–2070 (2014).

18. Chen, N. H., Djoko, K. Y., Veyrier, F. J. & McEwan, A. G. Formaldehyde Stress Responses in Bacterial Pathogens. *Front. Microbiol.* **7**, 257 (2016).

19. Pontel, L. B. *et al.* Endogenous Formaldehyde Is a Hematopoietic Stem Cell Genotoxin and Metabolic Carcinogen. *Mol. Cell* **60**, 177–188 (2015).

20. Allaman, I., Bélanger, M. & Magistretti, P. J. Methylglyoxal, the dark side of glycolysis. *Front. Neurosci.* **9**, 23 (2015).

21. Miller, D. V., Ruhlin, M., Ray, W. K., Xu, H. & White, R. H. N5,N10-methylenetetrahydromethanopterin reductase from Methanocaldococcus jannaschii also serves as a methylglyoxal reductase. *FEBS Lett.* **591**, 2269–2278 (2017).

22. Dingler, F. A. *et al.* Two Aldehyde Clearance Systems Are Essential to Prevent Lethal Formaldehyde Accumulation in Mice and Humans. *Mol. Cell* **80**, 996–1012 (2020).

23. Li, Z., Xu, Y., Zhu, H. & Qian, Y. Imaging of formaldehyde in plants with a ratiometric fluorescent probe. *Chem. Sci.* **8**, 5616–5621 (2017).

24. Kimmerer, T. W. & Macdonald, R. C. Acetaldehyde and ethanol biosynthesis in leaves of plants. *Plant Physiol.* **84**, 1204–1209 (1987).

25. Quintanilla, M. E., Tampier, L., Sapag, A., Gerdtzen, Z. & Israel, Y. Sex differences, alcohol dehydrogenase, acetaldehyde burst, and aversion to ethanol in the rat: a systems perspective. *Am. J. Physiol. Endocrinol. Metab.* **293**, 531–537 (2007).

26. Yadav, S. K., Singla-Pareek, S. L., Ray, M., Reddy, M. K. & Sopory, S. K. Methylglyoxal levels in plants under salinity stress are dependent on glyoxalase I and glutathione. *Biochem. Biophys. Res. Commun.* **337**, 61–67 (2005).

27. Rabbani, N. & Thornalley, P. J. Measurement of methylglyoxal by stable isotopic dilution analysis LC-MS/MS with corroborative prediction in physiological samples. *Nat. Protoc.* **9**, 1969–1979 (2014).

28. Wang, M. *et al.* PDC1, a pyruvate/α-ketoacid decarboxylase, is involved in acetaldehyde, propanal and pentanal biosynthesis in melon (Cucumis melo L.) fruit. *Plant J.* **98**, 112–125 (2019).

29. Baskaran, S., Rajan, D. P. & Balasubramanian, K. A. Formation of methylglyoxal by bacteria isolated from human faeces. *J. Med. Microbiol.* **28**, 211–215 (1989).

30. Fujishige, N. *et al.* A novel Arabidopsis gene required for ethanol tolerance is conserved among plants and archaea. *Plant Cell Physiol.* **45**, 659–666 (2004).

31. Hirayama, T. *et al.* A novel ethanol-hypersensitive mutant of Arabidopsis. *Plant Cell Physiol.* **45**, 703–711 (2004).

32. Wydau, S., Ferri-Fioni, M. L., Blanquet, S. & Plateau, P. GEK1, a gene product of Arabidopsis thaliana involved in ethanol tolerance, is a D-aminoacyl-tRNA deacylase. *Nucleic Acids Res.* **35**, 930–938 (2007).

33. Calendar, R. & Berg, P. d-Tyrosyl RNA: Formation, hydrolysis and utilization for protein synthesis. *J. Mol. Biol.* **26**, 39–54 (1967).

34. Soutourina, J., Plateau, P., Delort, F., Peirotes, A. & Blanquet, S. Functional characterization of the D-Tyr-tRNA(Tyr) deacylase from Escherichia coli. *J. Biol. Chem.* **274**, 19109–19114 (1999).

35. Soutourina, J., Plateau, P. & Blanquet, S. Metabolism of D-aminoacyl-tRNAs in Escherichia coli and Saccharomyces cerevisiae cells. *J. Biol. Chem.* **275**, 32535–32542 (2000).

36. Kuncha, S. K., Kruparani, S. P. & Sankaranarayanan, R. Chiral checkpoints during protein biosynthesis. *J. Biol. Chem.* **294**, 16535–16548 (2019).

37. Kumar, P., Bhatnagar, A. & Sankaranarayanan, R. Chiral proofreading during protein biosynthesis and its evolutionary implications. *FEBS Lett.* **13**, 1615–1627 (2022).

38. Ferri-Fioni, M. L. *et al.* Identification in archaea of a novel D-Tyr-tRNATyr deacylase. *J. Biol. Chem.* **281**, 27575–27585 (2006).

39. Wydau, S., van der Rest, G., Aubard, C., Plateau, P. & Blanquet, S. Widespread distribution of cell defense against D-aminoacyl-tRNAs. *J. Biol. Chem.* **284**, 14096–14104 (2009).

40. Mazeed, M. *et al.* Recruitment of archaeal DTD is a key event toward the emergence of land plants. *Sci. Adv.* **7**, eabe8890 (2021).

41. Kumar, P. *et al.* Distinct localization of chiral proofreaders resolves organellar translation conflict in plants. *Proc. Natl. Acad. Sci. U. S. A.* **120**, e2219292120 (2023).

42. LoPachin, R. M. & Gavin, T. Molecular Mechanisms of Aldehyde Toxicity: A Chemical Perspective. *Chem. Res. Toxicol.* **27**, 1081–1091 (2014).

43. Pratihar, S. Electrophilicity and nucleophilicity of commonly used aldehydes. *Org. Biomol. Chem.* **12**, 5781–5788 (2014).

44. Welchen, E. *et al.* d-Lactate Dehydrogenase Links Methylglyoxal Degradation and Electron Transport through Cytochrome c. *Plant Physiol.* **172**, 901–912 (2016).

45. Wienstroer, J., Engqvist, M. K. M., Kunz, H. H., Flügge, U. I. & Maurino, V. G. d-

Lactate dehydrogenase as a marker gene allows positive selection of transgenic plants. *FEBS Lett.* **586**, 36–40 (2012).

46. Achkor, H. *et al.* Enhanced Formaldehyde Detoxification by Overexpression of Glutathione-Dependent Formaldehyde Dehydrogenase from Arabidopsis. *Plant Physiol.* **132**, 2248–2255 (2003).

47. Zhu, J. K. Abiotic Stress Signaling and Responses in Plants. *Cell* **167**, 313–324 (2016).

48. Bucher, M., Brändle, R. & Kuhlemeier, C. Ethanolic fermentation in transgenic tobacco expressing Zymomonas mobilis pyruvate decarboxylase. *EMBO J.* **13**, 2755–2763 (1994).

49. Gupta, B. K. *et al.* Manipulation of glyoxalase pathway confers tolerance to multiple stresses in rice. *Plant. Cell Environ.* **41**, 1186–1200 (2018).

50. Zhao, J., Missihoun, T. D. & Bartels, D. The role of Arabidopsis aldehyde dehydrogenase genes in response to high temperature and stress combinations. *J. Exp. Bot.* **68**, 4295–4308 (2017).

51. Nurbekova, Z. *et al.* Arabidopsis aldehyde oxidase 3, known to oxidize abscisic aldehyde to abscisic acid, protects leaves from aldehyde toxicity. *Plant J.* **108**, 1439–1455 (2021).

52. Rodrigues, S. M. *et al.* Arabidopsis and tobacco plants ectopically expressing the soybean antiquitin-like ALDH7 gene display enhanced tolerance to drought, salinity, and oxidative stress. *J. Exp. Bot.* **57**, 1909–1918 (2006).

53. Odell, J. T., Nagy, F. & Chua, N.-H. Identification of DNA sequences required for activity of the cauliflower mosaic virus 35S promoter. *Nature* **313**, 810–812 (1985).

54. Seo, D. H., Seomun, S., Choi, Y. Do & Jang, G. Root Development and Stress Tolerance in rice: The Key to Improving Stress Tolerance without Yield Penalties. *Int. J. Mol. Sci.* **21**, 1807 (2020).

55. Tola, A. J., Jaballi, A., Germain, H. & Missihoun, T. D. Recent Development on Plant Aldehyde Dehydrogenase Enzymes and Their Functions in Plant Development and Stress Signaling. *Genes.* **12**, 51 (2020).

56. Islam, M. S. & Ghosh, A. Evolution, family expansion, and functional diversification of plant aldehyde dehydrogenases. *Gene* **829**, 146522 (2022).

57. Singla-Pareek, S. L., Kaur, C., Kumar, B., Pareek, A. & Sopory, S. K. Reassessing plant glyoxalases: large family and expanding functions. *New Phytol.* **227**, 714–721 (2020).

58. Xu, M. *et al.* Identification and molecular evolution of the GLX genes in 21 plant species: a focus on the Gossypium hirsutum. *BMC Genomics* **24**, 474 (2023).

59. Kanehisa, M., Sato, Y., Kawashima, M., Furumichi, M. & Tanabe, M. KEGG as a reference resource for gene and protein annotation. *Nucleic Acids Res.* **44**, D457–D462 (2016).

60. Wu, H. C., Bulgakov, V. P. & Jinn, T. L. Pectin Methylesterases: Cell Wall Remodeling Proteins Are Required for Plant Response to Heat Stress. *Front. Plant Sci.* **90**, 1612 (2018).

61. Dorokhov, Y. L., Sheshukova, E. V. & Komarova, T. V. Methanol in plant life. *Front. Plant Sci.* **9**, 1623 (2018).

62. Jarvis, M. C., Forsyth, W. & Duncan, H. J. A Survey of the Pectic Content of Nonlignified Monocot Cell Walls. *Plant Physiol.* **88**, 309 (1988).

63. Kessler, A. & Kalske, A. Plant Secondary Metabolite Diversity and Species Interactions. *Annu. Rev. Ecol. Evol. Syst.* **49**, 115–138 (2018).

64. Atherly, A. G. Peptidyl-transfer RNA hydrolase prevents inhibition of protein synthesis initiation. *Nature* **275**, 769–769 (1978).

65. Teiri, H., Pourzamzni, H. & Hajizadeh, Y. Phytoremediation of Formaldehyde from Indoor Environment by Ornamental Plants: An Approach to Promote Occupants Health. *Int. J. Prev. Med.* **9**, 70 (2018).

66. Aydogan, A. & Montoya, L. D. Formaldehyde removal by common indoor plant species and various growing media. *Atmos. Environ.* **45**, 2675–2682 (2011).

67. Wang, Z., Pei, J. & Zhang, J. S. Experimental investigation of the formaldehyde removal mechanisms in a dynamic botanical filtration system for indoor air purification. *J. Hazard. Mater.* **280**, 235–243 (2014).

68. Li, J., Xie, C. J., Cai, J., Yan, L. S. & Lu, M. M. Removal of Low-Molecular Weight Aldehydes by Selected Houseplants under Different Light Intensities and CO2 Concentrations. *Atmosphere.* **7**, 144 (2016).

69. Quimio, C. A. *et al.* Enhancement of Submergence Tolerance in Transgenic Rice Overproducing Pyruvate Decarboxylase. *J. Plant Physiol.* **4**, 516–521 (2000).

70. Su, W. *et al.* The alcohol dehydrogenase gene family in sugarcane and its involvement in cold stress regulation. *BMC Genomics* **21**, 1–17 (2020).

71. Sun, Y. *et al.* Overexpression of TaBADH increases salt tolerance in Arabidopsis. *Can. J. Plant Sci.* **99**, 546–555 (2019).

72. Kitadai, N. & Maruyama, S. Origins of building blocks of life: A review. *Geosci. Front.* **9**, 1117–1153 (2018).

73. Miller, S. L. & Urey, H. C. Organic compound synthesis on the primitive earth. *Science* **130**, 245–251 (1959).

74. Miller, S. L. The mechanism of synthesis of amino acids by electric discharges. *Biochim. Biophys. Acta* **23**, 480–489 (1957).

75. Parker, E. T. *et al.* Primordial synthesis of amines and amino acids in a 1958 Miller H2S-rich spark discharge experiment. *Proc. Natl. Acad. Sci. U. S. A.* **108**, 5526–5531 (2011).

76. Naraoka, H. *et al.* Soluble organic molecules in samples of the carbonaceous asteroid (162173) Ryugu. *Science.* **379**, eabn9033 (2023).

77. Moran, J. J. *et al.* Formaldehyde as a carbon and electron shuttle between autotroph and heterotroph populations in acidic hydrothermal vents of Norris Geyser Basin, Yellowstone National Park. *Extremophiles* **20**, 291–299 (2016).

78. Gribaldo, S. & Brochier-Armanet, C. The origin and evolution of Archaea: a state of

the art. *Philos. Trans. R. Soc. B Biol. Sci.* **361**, 1007 (2006).

79. Merino, N. *et al.* Living at the Extremes: Extremophiles and the Limits of Life in a Planetary Context. *Front. Microbiol.* **10**, 780 (2019).

80. Spang, A., Caceres, E. F. & Ettema, T. J. G. Genomic exploration of the diversity, ecology, and evolution of the archaeal domain of life. *Science* **357**, 6351 (2017).

81. Taffner, J. *et al.* What Is the Role of Archaea in Plants? New Insights from the Vegetation of Alpine Bogs. *mSphere* **3**, e00122-18 (2018).

82. Vranova, V. *et al.* The significance of D-amino acids in soil, fate and utilization by microbes and plants: review and identification of knowledge gaps. *Plant Soil* **354**, 21–39 (2011).

83. Kharanzhevskaya, Y. A., Voistinova, E. S. & Ivanova, E. S. Chemical composition and quality of bog waters in the Chaya river basin. *Contemp. Probl. Ecol.* **4**, 100–105 (2011).

84. Borysiuk, K., Ostaszewska Bugajska, M., Vaultier, M. N., Hasenfratz Sauder, M. P. & Szal, B. Enhanced Formation of Methylglyoxal-Derived Advanced Glycation End Products in Arabidopsis Under Ammonium Nutrition. *Front. Plant Sci.* **9**, 667 (2018).

85. Clough, S. J. & Bent, A. F. Floral dip: a simplified method for Agrobacterium-mediated transformation of Arabidopsis thaliana. *Plant J.* **16**, 735–743 (1998).

86. Van Den Ent, F. & Löwe, J. RF cloning: A restriction-free method for inserting target genes into plasmids. *J. Biochem. Biophys. Methods* **67**, 67–74 (2006).

87. Ahmad, S. *et al.* Mechanism of chiral proofreading during translation of the genetic code. *Elife* **2**, e01519 (2013).

88. Ledoux, S. & Uhlenbeck, O. C. [3′-32P]-labeling tRNA with nucleotidyltransferase for assaying aminoacylation and peptide bond formation. *Methods* **44**, 74–80 (2008).

89. Kuncha, S. K. *et al.* A chiral selectivity relaxed paralog of DTD for proofreading tRNA mischarging in Animalia. *Nat. Commun.* **9**, 511 (2018).

Figures and Tables

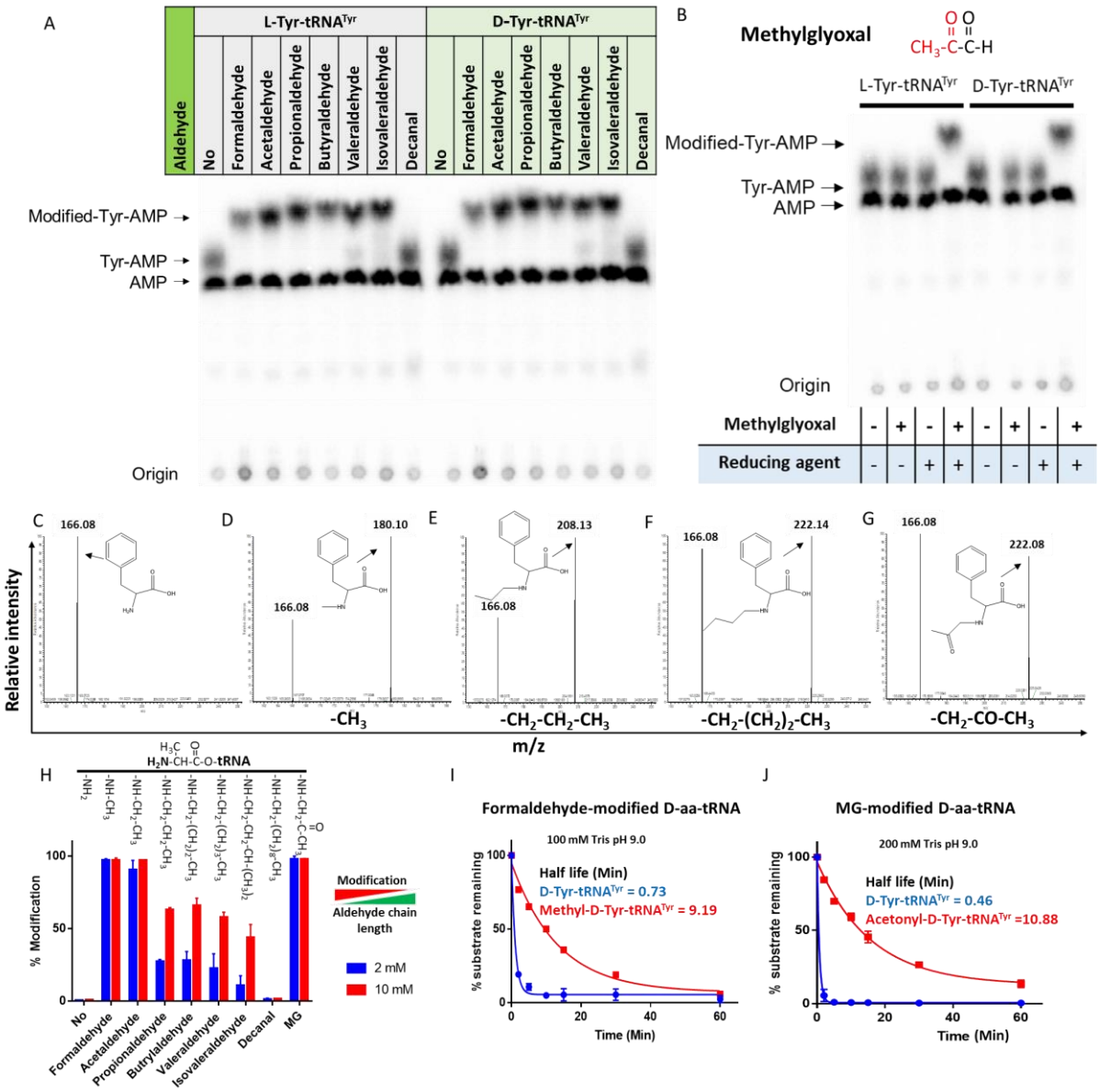

Fig 1. Aldehydes generate N-alkylated-aa-tRNA adducts.

TLC showing modification on L- and D-Tyr-tRNA^{Tyr} by A) formaldehyde, acetaldehyde, propionaldehyde, butyraldehyde, valeraldehyde, isovaleraldehyde, decanal and B) MG (AMP: adenine mono phosphate which corresponds to free tRNA; whereas Tyr-AMP and Modified-Tyr-AMP corresponds to unmodified and modified Tyr-tRNA^{Tyr}). These modifications were generated by incubating 2 µM aa-tRNA with 100 mM of respective aldehydes along with 20 mM Sodium cyanoborohydride (in 100 mM Potassium acetate (pH 5.4)) as a reducing agent at 37°C for 30 mins. Mass spectra showing C) D-Phe-tRNA^{Phe}, D) formaldehyde modified D-Phe-tRNA^{Phe} E) propionaldehyde modified D-Phe-tRNA^{Phe} F) Butyraldehyde modified D-Phe-

tRNA^{Phe} G) MG modified D-Phe-tRNA^{Phe}. H) Graph showing the effect of increasing chain length of aldehyde on modification propensity with aa-tRNA at two different concentrations of various aldehydes. Effect of I) formaldehyde, and J) MG modification on stability of ester linkage in D-aa-tRNA under alkaline conditions.

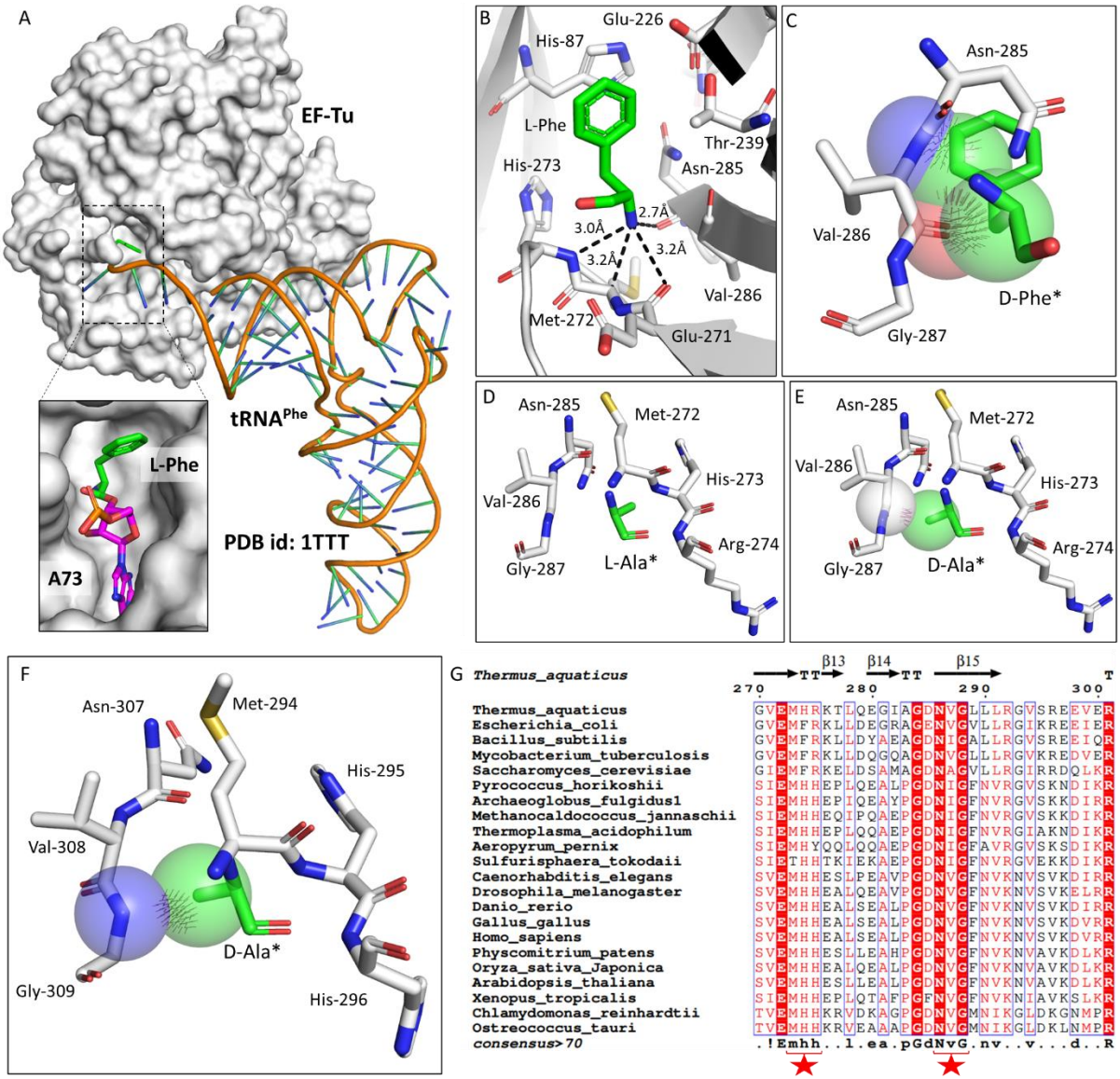

Fig 2. Elongation factor enantioselects aa-tRNAs through D-chiral rejection mechanism

A) Surface representation showing the cocrystal structure of EF-Tu with L-Phe-tRNA^{Phe}. Zoomed-in image showing the binding of L-phenylalanine with side chain projected outside of binding site of EF-Tu (PDB id: 1TTT). B) Zoomed-in image of amino acid binding site of EF-Tu bound with L-phenylalanine showing the selection of amino group of amino acid through main chain atoms (PDB id: 1TTT). C) Modelling of D-phenylalanine in the amino acid binding site of EF-Tu shows severe clashes with main chain atoms of EF-Tu. Modelling of smallest chiral amino acid, alanine, in the amino acid binding site of EF-Tu shows D) no clashes with L-alanine and E) clashes with D-alanine. F) Modelling of D-alanine in the amino acid binding site of eEF-1A shows clashes with main chain atoms. (*Represents modelled molecule). G) Structure-based sequence alignment of elongation factor from bacteria, archaea and eukaryotes

(both plants and animals) showing conserved amino acid binding site residues. (Key residues are marked with red star).

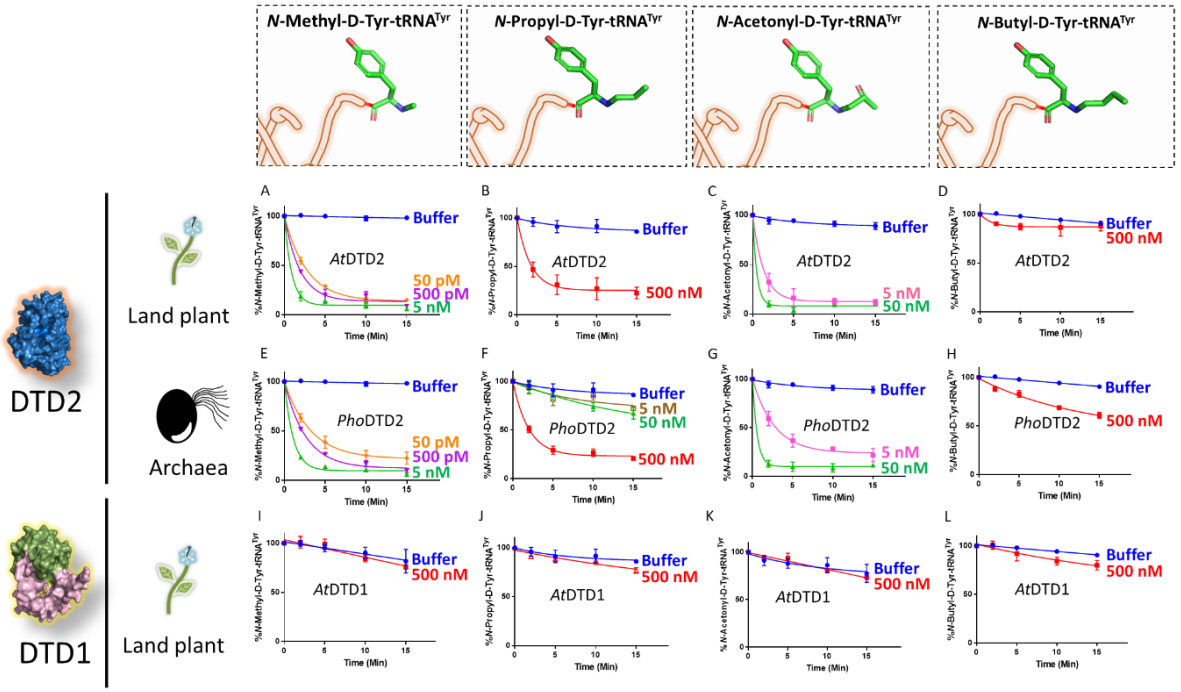

M

Aldehyde	Modification	*At*DTD2	*Pho*DTD2	*At*DTD1	Archaeal PTH	Bacterial PTH
Formaldehyde	$-CH_3$	50 pM	50 pM	-	-	-
Acetaldehyde*	$-CH_2-CH_3$	500 pM	500 pM	-	-	-
Methylglyoxal	$-CH_2-CO-CH_3$	5 nM	5 nM	-	-	-
Propionaldehyde	$-CH_2-CH_2-CH_3$	500 nM	500 nM	-	-	-
Butyraldehyde	$-CH_2-(CH_2)_2-CH_3$	-	-	-	-	-
Valeraldehyde	$-CH_2-(CH_2)_3-CH_3$	-	-	-	-	-

Fig 3. DTD2 acts as a general aldehyde detoxification system

Deacylation assays on formaldehyde, propionaldehyde, methylglyoxal and butyraldehyde modified D-Tyr-tRNA^{Tyr} substrates by *At*DTD2 (A-D), *Pho*DTD2 (E-H), *At*DTD1 (I-L): M) Table showing the effective activity concentration of *At*DTD2, *Pho*DTD2, *At*DTD1, archaeal PTH and bacterial PTH that completely deacylates aldehyde modified D-Tyr-tRNA^{Tyr} ('-' denotes no activity; *from Mazeed et al.[40]).

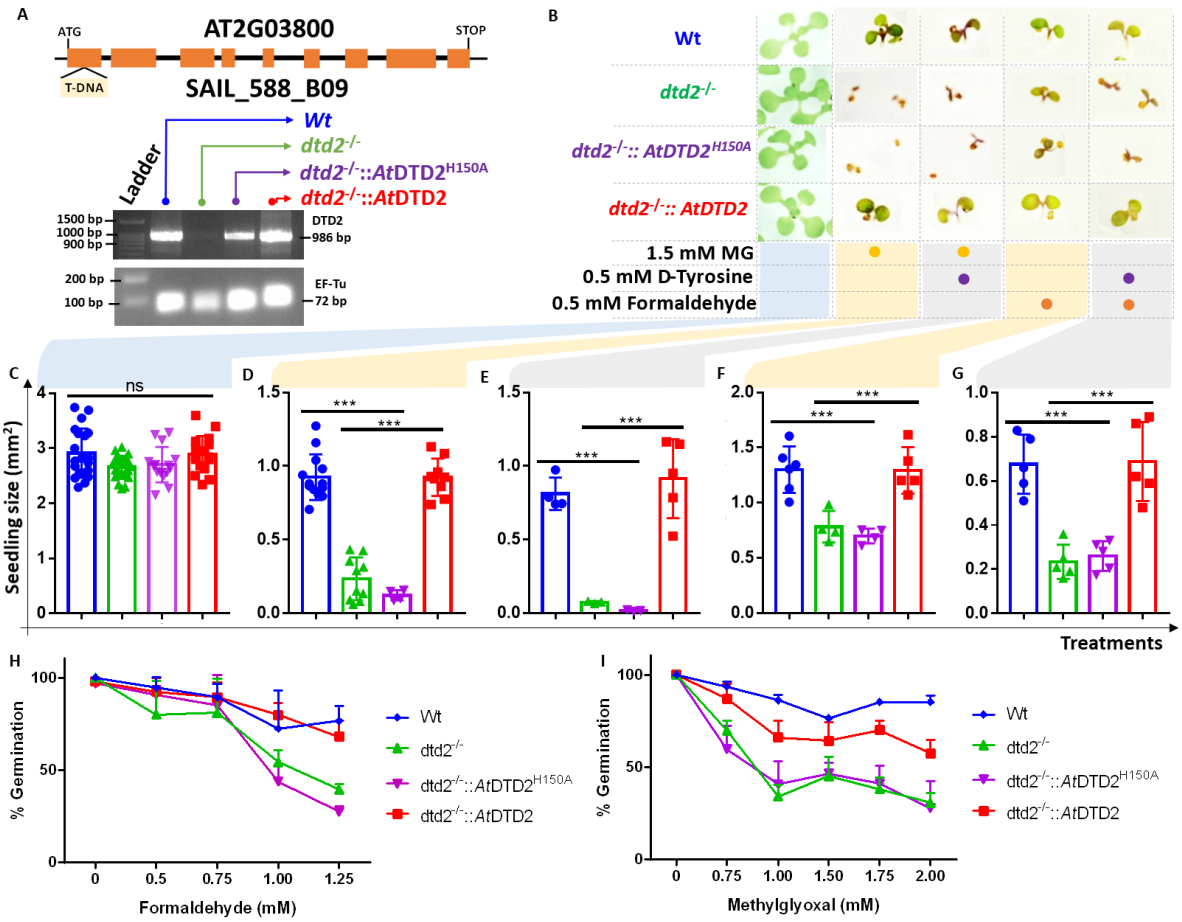

730

731 **Fig 4. DTD2 mutant plants are susceptible to physiologically abundant toxic aldehydes**

732 A) Schematics showing the site of T-DNA insertion in (SAIL_288_B09) the first exon of
733 DTD2 gene and RT-PCR showing the expression of DTD2 gene in wildtype (Wt), *dtd2*$^{-/-}$, *dtd2*$^{-}$
734 $^{/-}$*::At*DTD2 (rescue) and *dtd2*$^{-/-}$*::At*DTD2 H150A (catalytic mutant) plants lines used in the
735 study. B) Toxicity assays showing the effect of formaldehyde and MG with and without D-
736 amino acid (D-Tyrosine (D-Tyr)) on *dtd2*$^{-/-}$ plants. Graph showing effect of C) Murashige and
737 Skoog agar (MSA), D) 1.5 mM MG, E) 0.5 mM D-Tyr and 1.5 mM MG, F) 0.5 mM
738 formaldehyde and G) 0.5 mM D-Tyr and 0.5 mM formaldehyde on growth of Wt (Blue), *dtd2*$^{-}$
739 $^{/-}$ (Green), *dtd2*$^{-/-}$*::*AtDTD2 H150A (catalytic mutant) (Purple), and *dtd2*$^{-/-}$*::At*DTD2 (rescue)
740 (Red) plants. Cotyledon surface area (mm^2) is plotted as parameter for seedling size (n=4-15).
741 P values higher than 0.05 are denoted as ns and P $\leq$ 0.001 are denoted as ***. Graph showing
742 effect of H) formaldehyde and I) MG on germination of Wt, *dtd2*$^{-/-}$, *dtd2*$^{-/-}$*::At*DTD2 (rescue)
743 and *dtd2*$^{-/-}$*::At*DTD2 H150A (catalytic mutant) plants.

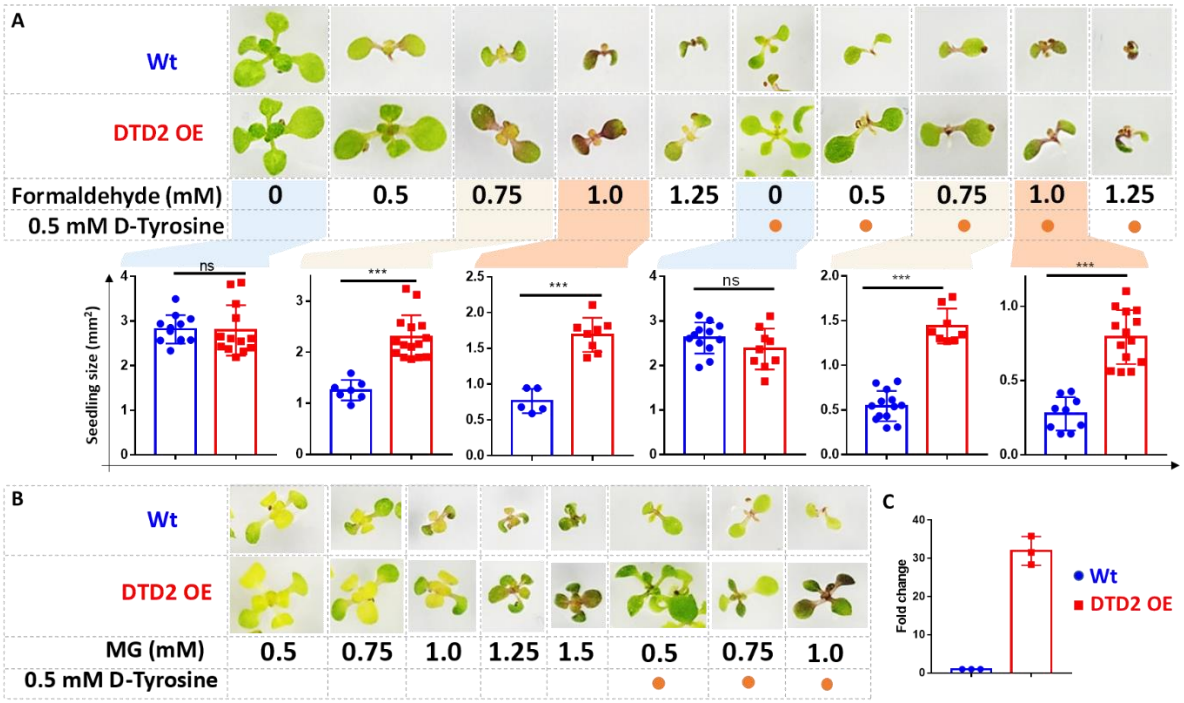

Fig 5. Overexpression of DTD2 confers increased multi aldehyde tolerance to *Arabidopsis thaliana*.

DTD2 overexpression (OE) plants grow better than wild type Col-0 under A) 0.5 mM, 0.75 mM, 1.0 mM and 1.25 mM of formaldehyde with and without 0.5 mM D-tyrosine. Cotyledon surface area (mm^2) is plotted as parameter for seedling size (n=5-15); P values higher than 0.05 are denoted as ns and $P \leq 0.001$ are denoted as ***. B) Growth of DTD2 OE and wild type Col-0 under 0.5 mM, 0.75 mM, 1.0 mM, 1.25 mM, 1.5 mM of MG and 0.5 mM, 0.75 mM, 1.0 mM MG with 0.5 mM D-tyrosine. C) The qPCR analysis showing fold change of DTD2 gene expression in DTD2 OE plant line used.

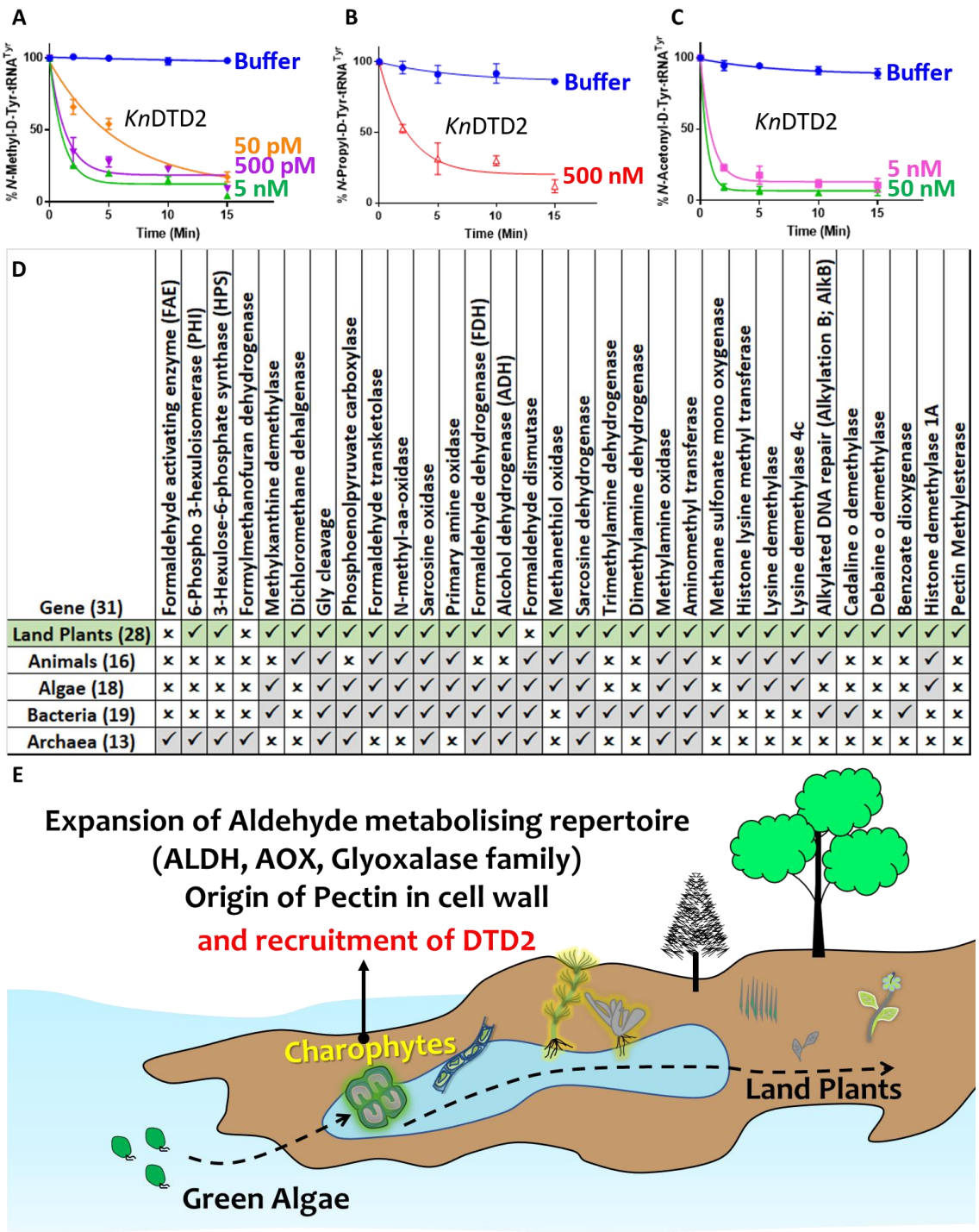

Gene (31)	Formaldehyde activating enzyme (FAE)	6-Phospho 3-hexuloisomerase (PHI)	3-Hexulose-6-phosphate synthase (HPS)	Formylmethanofuran dehydrogenase	Methylxanthine demethylase	Dichloromethane dehalgenase	Gly cleavage	Phosphoenolpyruvate carboxylase	Formaldehyde transketolase	N-methyl-aa-oxidase	Sarcosine oxidase	Primary amine oxidase	Formaldehyde dehydrogenase (FDH)	Alcohol dehydrogenase (ADH)	Formaldehyde dismutase	Methanethiol oxidase	Sarcosine dehydrogenase	Trimethylamine dehydrogenase	Dimethylamine dehydrogenase	Methylamine oxidase	Aminomethyl transferase	Methane sulfonate mono oxygenase	Histone lysine methyl transferase	Lysine demethylase	Lysine demethylase 4c	Alkylated DNA repair (Alkylation B; AlkB)	Cadaline o demethylase	Debaine o demethylase	Benzoate dioxygenase	Histone demethylase 1A	Pectin Methylesterase
Land Plants (28)	×	✓	✓	×	✓	✓	✓	✓	✓	✓	✓	✓	✓	✓	×	✓	✓	✓	✓	✓	✓	✓	✓	✓	✓	✓	✓	✓	✓	✓	✓
Animals (16)	×	×	×	×	×	✓	✓	×	✓	✓	✓	✓	×	×	✓	✓	✓	×	×	✓	✓	×	✓	✓	✓	✓	×	×	×	✓	×
Algae (18)	×	×	×	×	✓	×	✓	✓	✓	✓	✓	✓	✓	✓	✓	✓	✓	×	×	✓	✓	×	✓	✓	✓	×	×	×	×	✓	×
Bacteria (19)	×	×	×	×	✓	×	✓	✓	✓	✓	✓	✓	✓	✓	✓	×	✓	✓	✓	✓	✓	✓	×	×	×	✓	✓	×	✓	×	×
Archaea (13)	✓	✓	✓	✓	×	×	✓	✓	×	×	✓	×	✓	✓	✓	×	✓	×	×	✓	✓	×	×	×	×	×	×	×	×	×	×

Fig 6. Terrestrialization of plants is associated with expansion of aldehyde metabolising genes.

Deacylation assays of *Kn*DTD2 on A) formaldehyde, B) propionaldehyde and C) MG modified D-Tyr-tRNA^{Tyr}. D) Table showing the presence of 31 genes associated with formaldehyde metabolism in all KEGG organisms across life forms. E) Model showing the expansion of

aldehyde metabolising repertoire, cell wall components and recruitment of archaeal DTD2 in charophytes during land plant evolution.

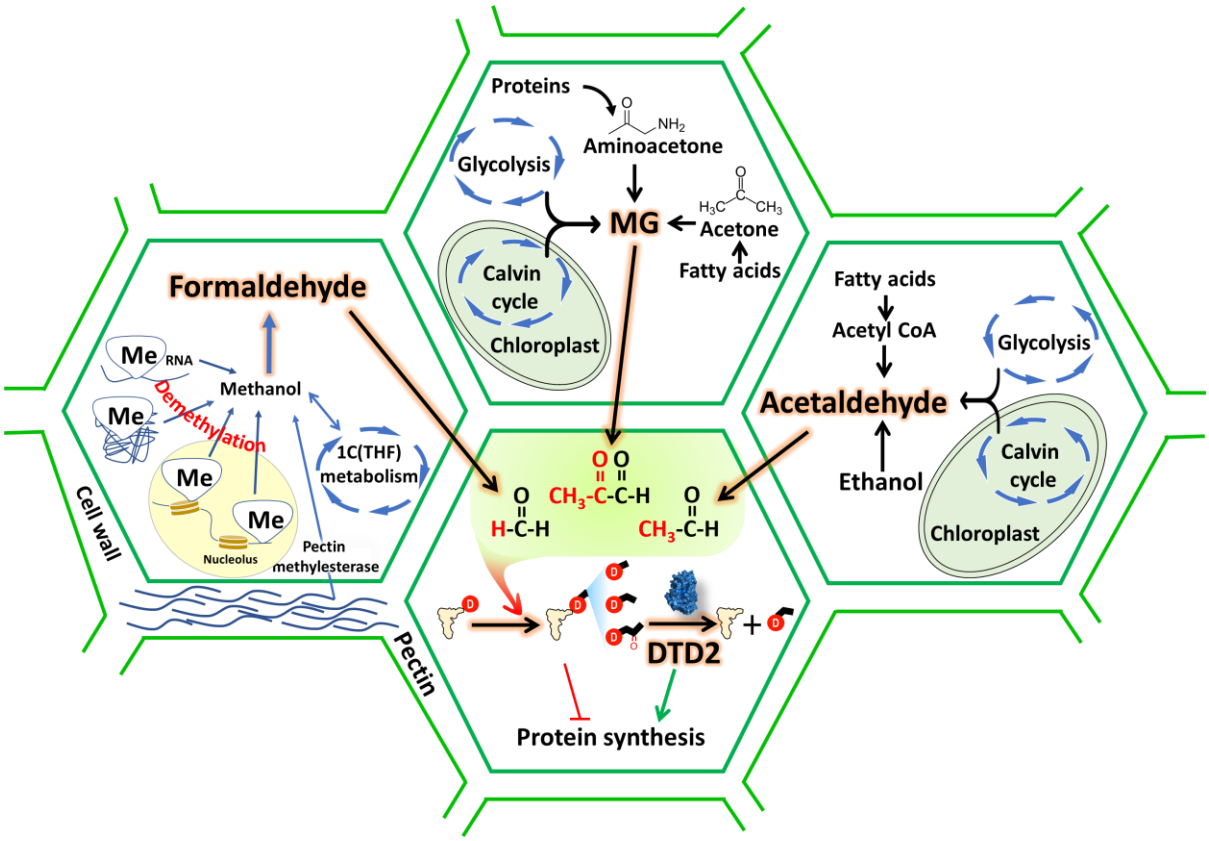

Fig 7. DTD2 acts as a general aldehyde detoxifier in land plants during translation quality control

Model showing the production of multiple aldehydes like formaldehyde, acetaldehyde and methylglyoxal (MG) through various metabolic processes in plants. These aldehydes generate stable alkyl modification on D-aminoacyl-tRNA adducts and DTD2 is unique proofreader for these alkyl adducts. Therefore, DTD2 protects plants from aldehyde toxicity associated with translation apparatus emerged from expanded metabolic pathways and D-amino acids.

Supporting Information for

Archaeal origin translation proofreader imparts multialdehyde stress tolerance to land plants

Pradeep Kumar[1,2,3], Ankit Roy[1], Shivapura Jagadeesha Mukul[1,2,3], Avinash Kumar Singh[1], Dipesh Kumar Singh[1], Aswan Nalli[1], Pujaita Banerjee[1], Kandhalu Sagadevan Dinesh Babu[1], Bakthisaran Raman[1], Shobha P. Kruparani[1], Imran Siddiqi[1,2], Rajan Sankaranarayanan[1,2,3*]

[1]CSIR–Centre for Cellular and Molecular Biology, Uppal Road, Hyderabad 500007, India.
[2]Academy of Scientific and Innovative Research (AcSIR), CSIR–CCMB campus, Uppal Road, Hyderabad 500007, India

[3]Academy of Scientific and Innovative Research (AcSIR), Ghaziabad- 201002, India

*Corresponding author. Email: sankar@ccmb.res.in (RS)

This file includes:

Figs. S1 to S8

Table S1

A

Chain length	Aldehyde	Organism	Levels (μM)	References
1-C	Formaldehyde	Opisthokont	4	Dingler et al., 2017
		Plants	~100-1000	Trézl et al., 1998; Li et al., 2017
2-C	Acetaldehyde	Plants	~200-1004	Kimmerer et al., 1987
		Opisthokont	15-20	Quintanilla González et al., 2007
3-C	Methylglyoxal	Plants	~70-200	Yadav et al., 2005
		Archaea	~70-2100	Miller et al., 2017
		Opisthokont	0.132-4.5	Rabbani et al., 2014
		Bacteria	25-142	Baskaran et al., 1989
3-C	Propionaldehyde	Plants	1-6	Wang et al., 2019
4-C	Butyraldehyde	Plants	0.8-2.8	Wang et al., 2019
5-C	Valeraldehdye	Plants	0.25-3	Wang et al., 2019

B

Aldehyde	Modification	Expected mass change (Da)	Observed mass change (Da)
Formaldehyde	$-CH_3$	14.015	14.015
Acetaldehyde	$-CH_2-CH_3$	28.031	28.032*
Methylglyoxal	$-CH_2-CO-CH_3$	56.026	56.026
Propionaldehyde	$-CH_2-CH_2-CH_3$	42.046	42.046
Butyraldehyde	$-CH_2-(CH_2)_2-CH_3$	56.062	56.062
Valeraldehdye	$-CH_2-(CH_2)_3-CH_3$	70.078	70.078

H

Molecule	Molecule Size		Modification Size	
	Volume (Å³)	Surface area (Å²)	Volume (Å³)	Surface area (Å²)
D-Ala	110	117	0	0
N-Methyl-D-Ala	135	135	25	18
N-Ethyl-D-Ala	160	158	50	41
N-Propyl-D-Ala	182	175	76	61
N-Acetonyl-D-Ala	186	178	72	58
N-Butryl-D-Ala	204	194	94	77
N-Valeryl-D-Ala	228	214	118	97

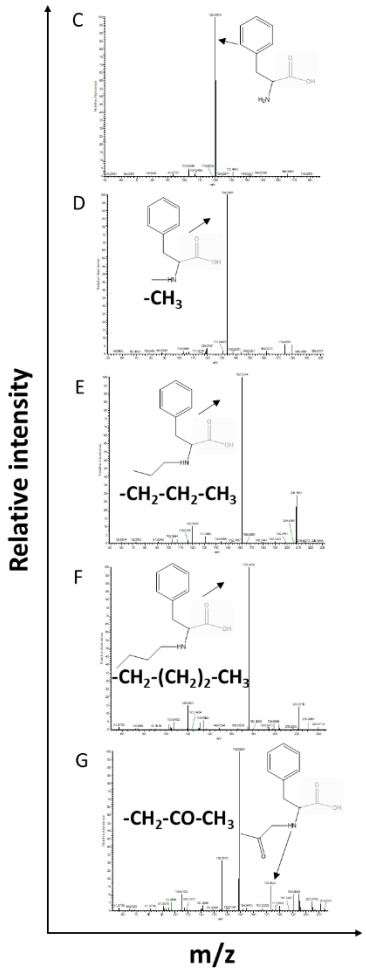

Fig S1. Aldehydes modify the amino group of amino acids in D-aa-tRNAs

A) Table showing the presence of various aldehydes in different domains of life[3,21–28]. B) Table showing modification type, expected and observed mass change by different aldehyde on D-aa-tRNA; *Mass change observed after acetaldehyde treatment in earlier study[40]. Tandem fragmentation mass spectra (MS^2) showing modification on the amino group of amino acid in C) D-Phe-$tRNA^{Phe}$, D) formaldehyde modified D-Phe-$tRNA^{Phe}$, E) propionaldehyde modified D-Phe-$tRNA^{Phe}$, F) butyraldehyde modified D-Phe-$tRNA^{Phe}$ and G) MG modified D-Phe-$tRNA^{Phe}$. H) Table showing the calculated molecular size and modification size (both volume $Å^3$ and surface area $Å^2$) by various aldehydes on D-amino acid (D-alanine) using the Voss Volume Voxelator (3V) webserver at probe 1.5 Å radius.

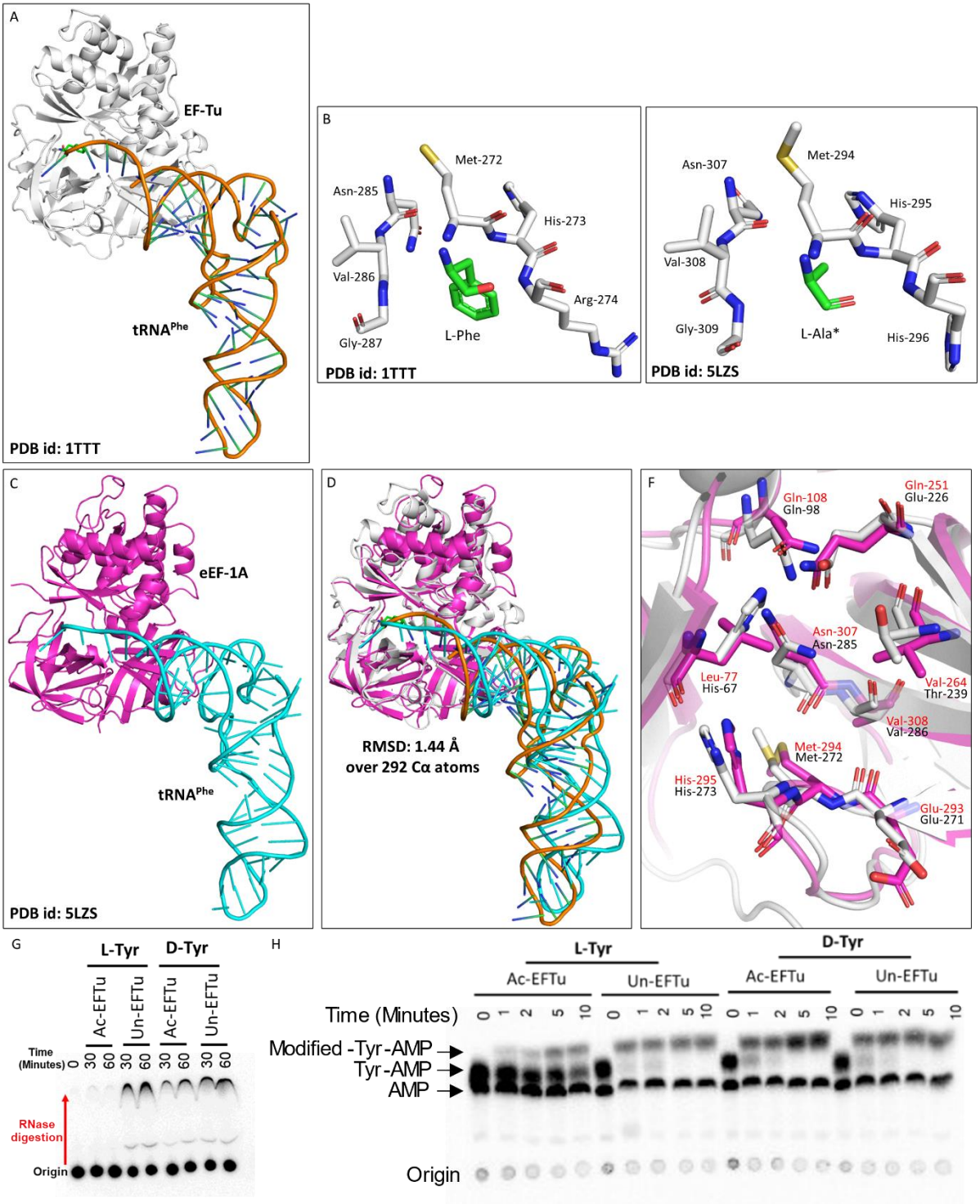

Fig S2. Elongation factor protects L-aa-tRNAs from aldehyde modification

A) Cartoon representation showing the cocrystal structure of EF-Tu with L-Phe-tRNA^{Phe} (PDB id: 1TTT). B) Zoomed-in image of amino acid binding site of EF-Tu bound with L-phenylalanine (PDB id: 1TTT). C) Cartoon representation showing the cryoEM structure of eEF-1A with tRNA^{Phe} (PDB id: 5LZS). D) Image showing the overlap of EF-Tu:L-Phe-

tRNA^{Phe} crystal structure and eEF-1A:tRNAPhe cryoEM structure (r.m.s.d. of 1.44 Å over 292 Cα atoms). E) Zoomed-in image of amino acid binding site of eEF-1A with modelled L-alanine (PDB id: 5ZLS). (*Modelled) F) Overlap showing the amino acid binding site residues of EF-Tu and eEF-1A. (EF-Tu residues are marked in black and eEF-1A residues are marked in red) G) Thin layer chromatography showing the activation profile of EF-Tu via RNase protection-based assay. H) Thin layer chromatography showing the formaldehyde modification on L- and D-aa-tRNAs in the presence of EF-Tu.

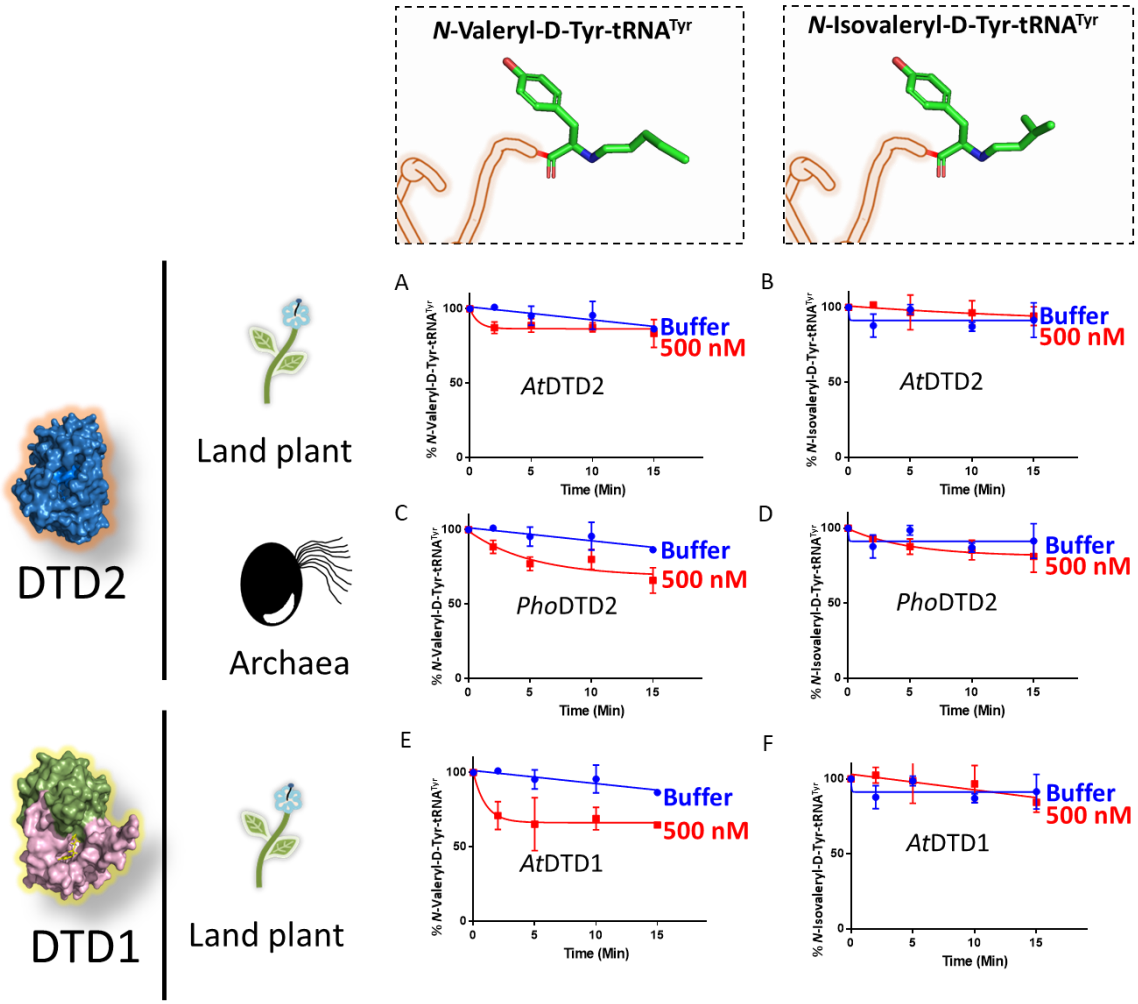

Fig S3. DTD2 is inactive on aldehyde-modified D-aa-tRNAs beyond three-carbon aldehyde chain length.

Deacylation assays of *At*DTD2 on A) valeraldehyde, B) isovaleraldehyde modified D-Tyr-tRNA^{Tyr}; Deacylation assays of *Pho*DTD2 on C) valeraldehyde, D) isovaleraldehyde modified D-Tyr-tRNA^{Tyr}; Deacylation assays of *At*DTD1 on E) valeraldehyde, F) isovaleraldehyde modified D-Tyr-tRNA^{Tyr}.

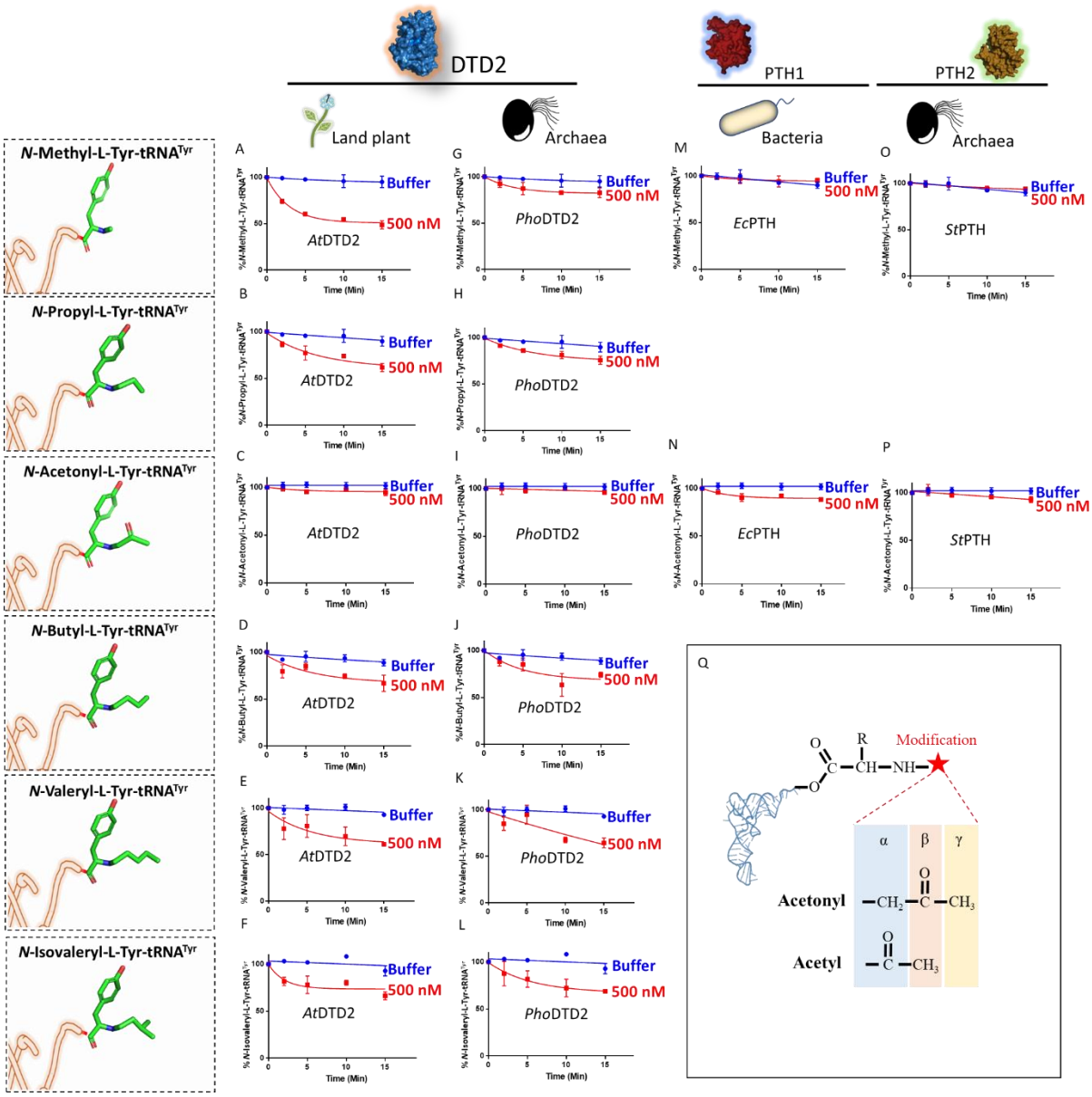

Fig S4. DTD2 acts as a general aldehyde detoxification system

Deacylation assays of *At*DTD2 on A) formaldehyde, B) propionaldehyde, C) MG, D) butyraldehyde, E) valeraldehyde, and F) isovaleraldehyde modified L-Tyr-tRNA^{Tyr}; Deacylation assays of *Pho*DTD2 on G) formaldehyde, H) propionaldehyde, I) MG, J) butyraldehyde, K) valeraldehyde, and L) isovaleraldehyde modified L-Tyr-tRNA^{Tyr}; Deacylation assays of *Ec*PTH on M) formaldehyde, and N) MG modified L-Tyr-tRNA^{Tyr}; Deacylation assays of *St*PTH on O) formaldehyde, and P) MG modified L-Tyr-tRNA^{Tyr}. Q) Figure showing the difference in the position of carbonyl carbon in acetonyl and acetyl modification on aa-tRNAs.

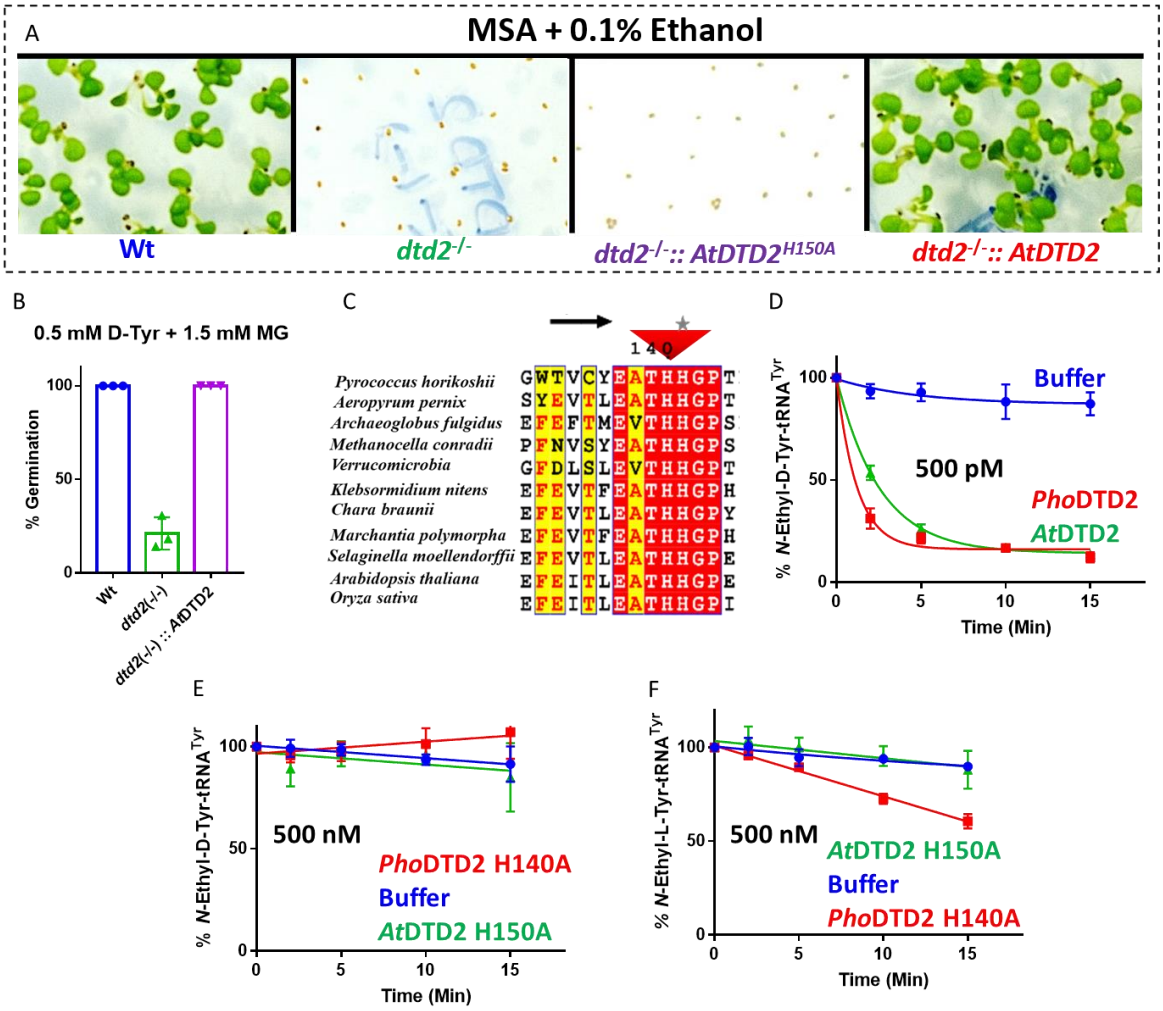

Fig S5. MG and formaldehyde inhibit the germination of DTD2 mutant plants

A) Toxicity assays showing the effect of 0.1% ethanol on wildtype (Wt), *dtd2*$^{-/-}$, *dtd2*$^{-/-}$*::At*DTD2 H150A (catalytic mutant) and *dtd2*$^{-/-}$*::At*DTD2 (rescue) plants B) Graph showing cumulative effect of MG and D-Tyrosine on germination of Col-0, *dtd2 (-/-)*, and *dtd2 (-/-)::At*DTD2 (rescue) plants. C) Structure based sequence alignment showing invariant catalytic histidine in evolutionarily distinct DTD2 sequences. Deacylation of D) acetaldehyde modified D-Tyr-tRNA^{Tyr} with *Pho*DTD2 and *At*DTD2. E) *Pho*DTD2 H140A and *At*DTD2 H150A (catalytic mutants) and F) Deacylation of acetaldehyde modified L-Tyr-tRNA^{Tyr} with *Pho*DTD2 H140A and *At*DTD2 H150A (catalytic mutants).

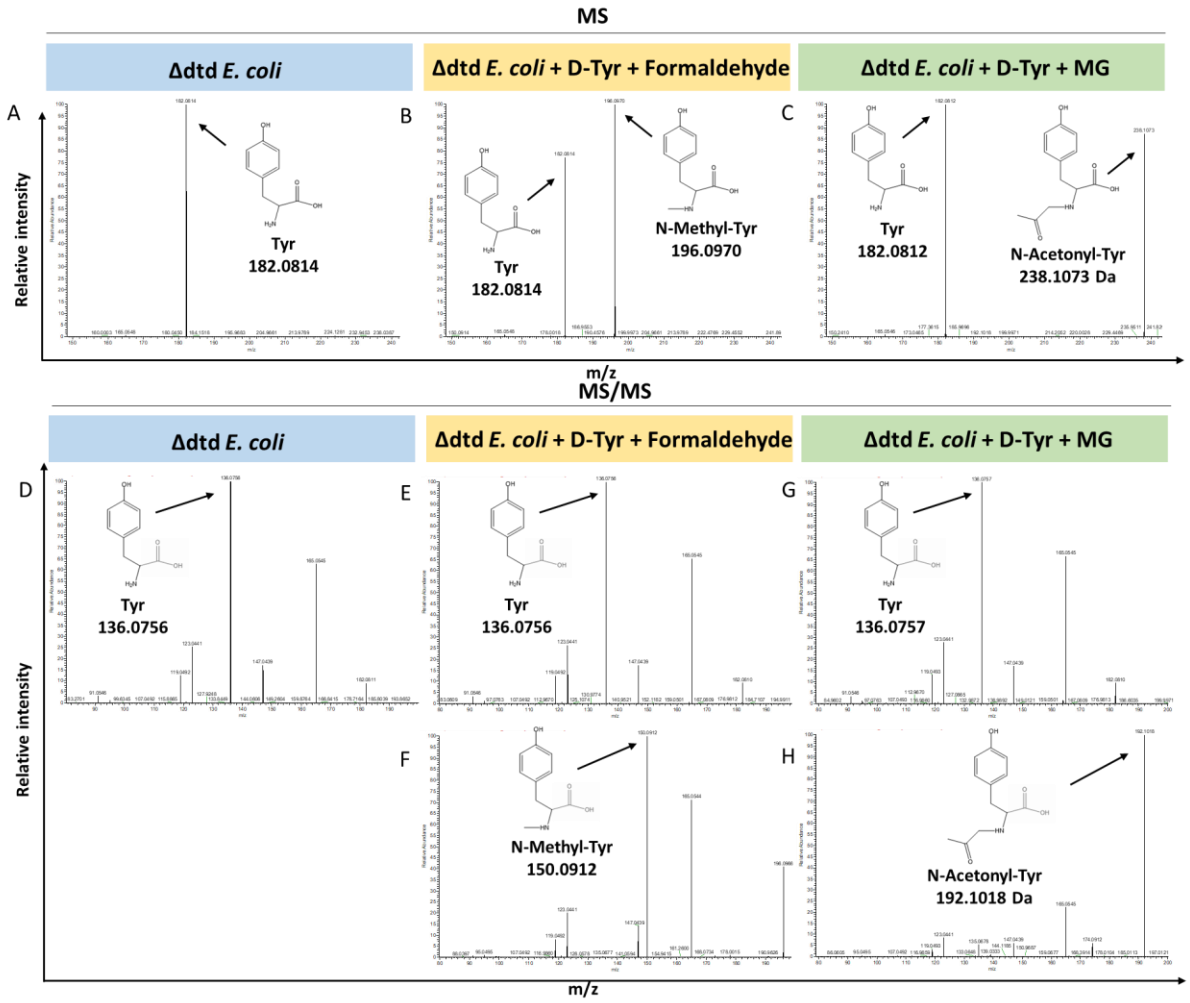

Fig S6. Loss of DTD results in accumulation of modified D-aminoacyl adducts on tRNAs in *E. coli*.

Mass spectrometry analysis showing the accumulation of aldehyde modified D-Tyr-tRNA^{Tyr} in A) Δdtd *E. coli*, B) formaldehyde and D-tyrosine treated Δdtd *E. coli*, and C) MG and D-tyrosine treated Δdtd *E. coli*. ESI-MS based tandem fragmentation analysis for unmodified and aldehyde modified D-Tyr-tRNA^{Tyr} in D) Δdtd *E. coli*, E) and F) formaldehyde and D-tyrosine treated Δdtd *E. coli*, G) and H) MG and D-tyrosine treated Δdtd *E. coli*.

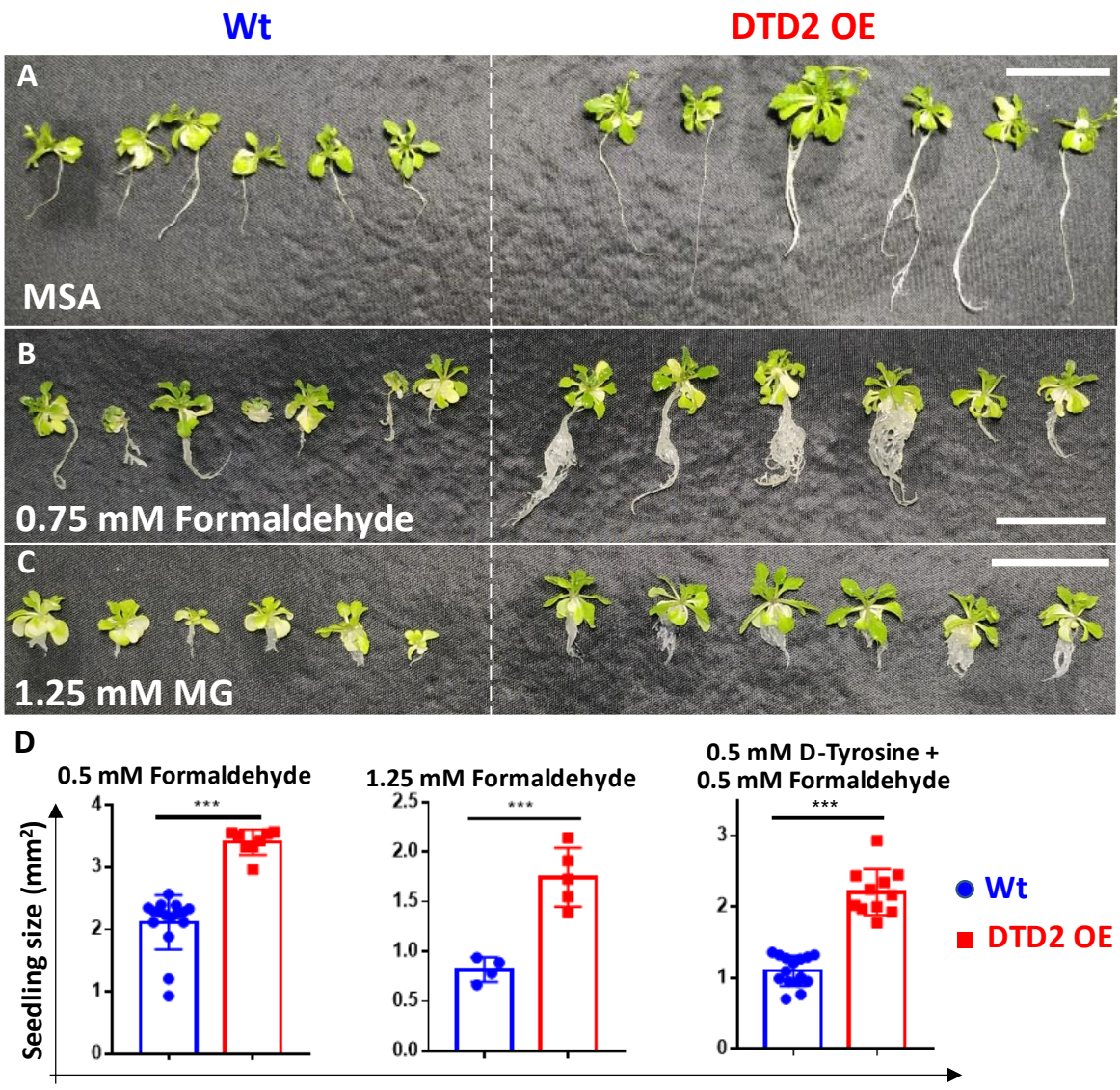

Fig S7. Overexpression of DTD2 confers multi aldehyde tolerance with D-amino acid stress in *Arabidopsis thaliana*.

DTD2 overexpression line grows better than wild type Col-0 under A) no stress, B) 0.75 mM formaldehyde and C) 1.25 mM MG. D) Graph showing the seedling size of Wt and DTD2 OE plants under 0.5 mM, 1.25 mM formaldehyde and 0.5 mM D-tyrosine with 0.5 mM formaldehyde. Cotyledon surface area (mm^2) is plotted as parameter for seedling size (n=4-15); P values higher than 0.05 are denoted as ns and $P \leq 0.001$ are denoted as ***.

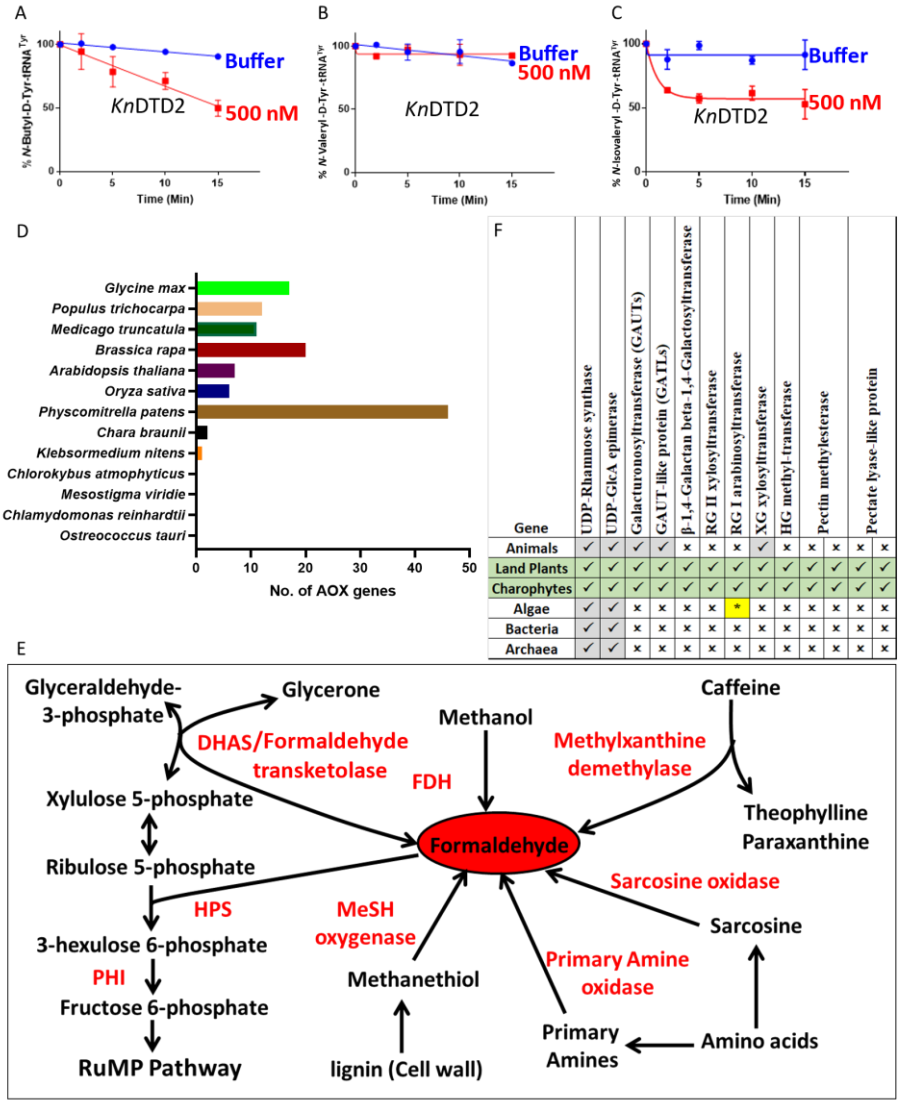

Fig S8. Land plant evolution is associated with the expansion of aldehyde metabolising repertoire.

Deacylation assays of *Kn*DTD2 on A) butyraldehyde, B) valeraldehyde, and C) isovaleraldehyde modified D-Tyr-tRNA^{Tyr}. D) Graph showing the number of genes for aldehyde oxidase (AOX) in viridiplantae. E) Schematics showing multiple enzymes involved in formaldehyde metabolism based on KEGG database across life forms. F) Table showing the

presence of enzymes involved in MG production in KEGG genomes of opisthokonts, land plants, algae, bacteria and archaea. Number denotes the percentage of KEGG organism encoding respective enzymes. G) Table showing the emergence of enzymes responsible for pectin biosynthesis and degradation in land plant ancestors. (*Present in few chlorophytes).

Table S1.

List of primers used in the study

At DTD2 N-His	FP	5' CCGCGCGGCAGCCATATGATGGTAACACTAATCGTGGCCA 3'
	RP	5' GTGGTGGTGGTGCTCGAGT TCATGTGAAATCGTTTGGCTTCC 3'
At DTD1 C-His	FP	5' TTAACTTTAAGAAGGAGATATACATATGATGAGAGCTGTAATCCAAAGAGT 3'
	RP	5' GTGGTGGTGCTCGAGTGCCTTGGTGGATTGAGGTGAGTC 3'
Pho DTD2 no tag	FP	5' TTTAAGAAGGAGATATACCATGGGCATGAAGGTCATAATGACGACTAAG 3'
	RP	5' CTCGAGTGCGGCCGCAAGCTTTTAATCCTTTATGAATTCCAAACCAAGTTC 3'
Ec PTH N-His	FP	5' CCGCGCGGCAGCCATATGATGACGATTAAATTGATTGTCG 3'
	RP	5' GTGGTGGTGGTGCTCGAGTTTATTGCGCTTTAAAGGCGTG 3'
St PTH N-His	FP	5' CGGCAGCCATATGGCTAGCATGGCTACTAAAATGGTAATAGTCGTAAGGAC 3'
	RP	5' CTCGAGTGCGGCCGCAAGCTTTTAAAGAAGTTTTAGATCTCCAGTTATCTTATCAAC 3'
At $tRNA^{Phe}$	FP	5' GCGGGGATAGCTCAGTTGGGAGAGCGTCAGACTGAAGATCTGAAGGTCGCGTGTTCGATCCACGCTCACCGCACCA 3'
	RP	5' TGGTGCGGTGAGCGTGGATCGAACACGCGACCTTCAGATCTTCAGTCTGACGCTCTCCCAACTGAGCTATCCCCGC 3'
At $tRNA^{Tyr}$	FP	5' CCGACCTTAGCTCAGTTGGTAGAGCGGAGGACTGTAGATCCTTAGGTCACTGGTTCGAATCCGGTAGGTCGGACCA 3'
	RP	5' TGGTCCGACCTACCGGATTCGAACCAGTGACCTAAGGATCTACAGTCCTCCGCTCTACCAACTGAGCTAAGGTCGG 3'
Pho $tRNA^{Tyr}$	FP	5' CCCGCGGTAGCCTAGCCTGGGAGTGGCGGCGGACTGTAGATCCGCAGGTCCCCGGTTCAAATCCGGGCCGCGGGACCA 3'
	RP	5' TGGTCCCGCGGCCCGGATTTGAACCGGGGACCTGCGGATCTACAGTCCGCCGCCACTCCCAGGCTAGGCTACCGCGGG 3'
Ec $tRNA^{Ala}$	FP	5' GGGGCTATAGCTCAGCTGGGAGAGCGCTTGCATGGCATGCAAGAGGTCAGCGGTTCGATCCCGCTTAGCTCCACCA 3'
	RP	5' TGGTGGAGCTAAGCGGGATCGAACCGCTGACCTCTTGCATGCCATGCAAGCGCTCTCCCAGCTGAGCTATAGCCCC 3'
DTD2 T-DNA insertion line (SAIL_588_B09)	LP	5' GACATATTCGGCTCATAATTTCAG 3’
	RP	5' TCAACCAAAACATCCTTCAGG 3’
	LB	5' GCCTTTTCAGAAATGGATAAATAGCCTTGCTTCC 3’
*At*DTD2 (RT-PCR)	Forward primer	5’- ACGCCAATAATCGCGTTACAGTAACAACTCG -3’
	Reverse primer	5’- TGTGAAATCGTTTGGCTTCCC -3’
At DTD2 (RT-qPCR)	FP	5' TGTTCATCCGATTGGAGTGCTTC 3’
	RP	5' ACCAATTCTAGTGCTTGGCAACG 3’
EF-Tu (RT-PCR)	Forward primer	5’- TCTGCCGCAGGTGAATCAAAGG -3’
	Reverse primer	5’- ACACAGACACGCGACCAAATACC -3’
Actin2 (AT3G18780) RT-qPCR	FP	5' TCTTCCGCTCTTTCTTTCCAAGC 3’
	RP	5' ACCATTGTCACACACGATTGGTTG 3’
At DTD2 genomic DNA with promotor	FP	5' GTAGTGGTTATCACGTTTGCC 3’
	RP	5' TCATGTGAAATCGTTTGGCTTCCCAACAT 3’
At DTD2 H150A	FP	5' CATTGGAAGCTACTGCTCATGGACCAATAACTAACAAG 3’
	RP	5' GTTAGTTATTGGTCCATGAGCAGTAGCTTCCAATGTTATC 3’
At DTD2 cDNA	FP	5' ATGATTTTGAAAATAAGCGGCCG 3’
	RP	5' TCATGTGAAATCGTTTGGCTTCCCAACAT 3’

DTD2 genotyping	SAIL_588_B 09 LP	5’-GACATATTCGGCTCATAATTTCAG 3’
	SAIL_588_B 09 RP	5’-TCAACCAAAACATCCTTCAGG 3’
	Sail LB3	5’-TAGCATCTGAATTTCATAACCAATCTCGATACAC 3’